INVESTIGATION OF GAS PHASE FRAGMENTATION REACTION MECHANISMS OF DOUBLY-PROTONATED b_n (n=7-9) IONS BY ION TRAP MASS SPECTROMETRY

A Thesis Submitted to
the Graduate School of Engineering and Science of
İzmir Institute of Technology
in Partial Fulfillment of the Requirements for the Degree of

MASTER OF SCIENCE

in Chemistry

by
Özge GÖRGÜN

December 2014
İZMİR

We approve the thesis of **Özge GÖRGÜN**

Examining Committee Members:

Prof. Dr. Nuran ELMACI IRMAK
Department of Chemistry, İzmir Institute of Technology

Assoc. Prof. Dr. Jens ALLMER
Department of Molecular Biology and Genetics, İzmir Institute of Technology

---

Prof. Dr. Talat YALÇIN
Department of Chemistry, İzmir Institute of Technology

17 December 2014

Prof. Dr. Talat YALÇIN
Supervisor, Department of Chemistry
İzmir Institute of Technology

Prof. Dr. Ahmet Emin EROĞLU
Head of the Department of Chemistry

Prof. Dr. Bilge KARAÇALI
Dean of the Graduate School
of Engineering and Sciences

ACKNOWLEDGEMENTS

I would like to thank my research advisor Prof. Dr. Talat YALÇIN for his guidance, support, understanding, patience and tolerance. It was an honor of me studying Biological Mass Spectrometry Laboratory leadership of him. I am also grateful to rest of my thesis committee Prof. Dr. Nuran ELMACI IRMAK and Assoc. Prof. Dr. Jens ALLMER.

I am appreciative of the financial support of The Scientific and Technological Research Council of Turkey (TÜBİTAK) for research project (Project No: 112T558).

Moreover, I would exclusively like to thank to my lab mate; Dr. A. Emin ATİK for his camaraderie, motivation, sharing his experience and knowledge whatever I need. I will always remain indebted for his familiar guidance. I would specially like to thank my other lab mates Melda Zeynep GÜRAY and Melike DİNÇ who became my cheerful sisters during this difficult period. It could be very difficult and unendurable without our commune to the accompaniment of drinking Turkish coffee. Furthermore, I am deeply grateful to Dr. Çağdaş TAŞOĞLU who has communicated with me for the first when I attended to the laboratory and has always helped me as a good friend. Besides, I would particularly like to thank Dr. Filiz YEŞİLIRMAK for moral support and her endless help both in laboratory and outdoor. And also, I am thankful to Dr. Sıla KARACA for his favor and friendliness.

Last but not least; I owe my endless thanks to my simple peerless family; my mother Resmiye GÖRGÜN, my father Halit GÖRGÜN and my brother Mert GÖRGÜN. I am sincerely a fortunate person, because it is incomparable that awake with a mother's smile of a full of love and feeling her compassion all the time, and feeling strong and safe because having an adoring father who is always near me for appreciate in successes and suggests in disappointments. As to my younger brother, life could be really unbearable without his ludicrousness different and also enlightening perspective to the experiences. Thank you very much for everything you have brought and will bring. I am the luckiest daughter and sister in the world as you help me laugh in the merciless life.

ABSTRACT

INVESTIGATION OF GAS PHASE FRAGMENTATION REACTION MECHANISMS OF DOUBLY-PROTONATED b_n (n=7-9) IONS BY ION TRAP MASS SPECTROMETRY

In this dissertation, the gas-phase fragmentation mechanisms of doubly-charged b_n (n=7, 8, and 9) ions from basic amino acid containing model peptides were investigated by means of collision-induced dissociation (CID) coupled tandem mass spectrometry (MS/MS). The study utilized two sets of C-terminal amidated model peptides that HYAGFLV-NH_2, YHAGFLV-NH_2, YAHGFLV-NH_2, YAGHFLV-NH_2, YAGFHLV-NH_2, YAGFLHV-NH_2, YAGFLVH-NH_2 and HAAAAAA-NH_2, AHAAAAA-NH_2, AAHAAAA-NH_2, AAAHAAA-NH_2, AAAAHAA-NH_2, AAAAAHA-NH_2, AAAAAAH-NH_2 where the position of the histidine (His) residue is varied from N-to-C-terminal. Both positional effect and peptide sequence effect were examined for the fragmentation reactions of doubly-protonated b_7 ions for these heptapeptides. The CID-MS^3 mass spectra of doubly-protonated b_7 ions have internal amino acid losses which provide an evidence for macrocyclization reaction. The proposed reaction mechanism involves charge-separation reaction of doubly-protonated *b* ions in the gas-phase which generates a protonated iminium ion of the N-terminal residue and protonated internal *b* ion with C-terminal oxazolone group. In addition to these model peptides, the C-terminal acid free forms of peptides such as SVEHAGVIL, SHIGDAVVI, EHAGVISVL, and GRIDKPILK were also used for to understand the extent of macrocyclization of doubly-charged b_8 ion and very similar results were obtained. Moreover, the C-terminal acid free forms of peptide KRNGVIIAGY were investigated for the behavior of doubly-protonated larger b_9 ion and doubly-protonated internal eliminations were obtained meanwhile singly-protonated amino acid eliminations and the mechanism was adjusted according to the results.

ÖZET

ÇİFTE PROTONLANMIŞ b_n (n=7-9) İYONLARININ GAZ FAZI PARÇALANMA REAKSİYON MEKANİZMALARININ İYON TUZAKLI KÜTLE SPEKTROMETRESİ İLE İNCELENMESİ

Bu tez, ardışık kütle spektrometresi ile birleştirilmiş çarpışmayla indüklenmiş ayrışma (CID) altında, bazik amino asit içeren model peptitlerden elde edilen çift-protonlanmış *b* iyonlarının gaz fazı parçalanma mekanizmalarının araştırılmasını içermektedir. Histidin amino asidinin konumunun, peptidin N-ucundan C-ucuna doğru değiştiği iki farklı peptit dizisi kullanılmıştır, bunlar şu şekilde isimlendirilir; HYAGFLV-NH_2, YHAGFLV-NH_2, YAHGFLV-NH_2, YAGHFLV-NH_2, YAGFHLV-NH_2, YAGFLHV-NH_2, YAGFLVH-NH_2 ve HAAAAAA-NH_2, AHAAAAA-NH_2, AAHAAAA-NH_2, AAAHAAA-NH_2, AAAAHAA-NH_2, AAAAAHA-NH_2, AAAAAAH-NH_2. Bazik amino asidin konumunun ve peptit dizilimlerinin, çift-protonlanmış *b* iyonlarının parçalanma reaksiyonları üzerindeki etkisi araştırılmıştır. Çift-protonlanmış *b* iyonlarının çarpışmayla-indüklenmiş ayrışma (CID) altında çok aşamalı ikili kütle spektrometresi (MS^3) spektrumlarında görülen içsel amino asit kopmaları, macrohalkalaşma tepkimesine kanıt teşkil etmektedir. Önerilen reaksiyon mekanizması, gaz fazındaki çifte-protonlanmış *b* iyonlarının yük-ayrımı reaksiyonu ile N-ucundan iminyum iyonları ve C-ucundaki okzazolon grubundan içsel *b* iyonları oluşturmasına dayanmaktadır. Adı geçen model peptitlere ek olarak C-ucu serbest asit içeren SVEHAGVIL, SHIGDAVVI, EHAGVISVL ve GRIDKPILK peptitleri kullanılarak çifte protonlanmış b_8 iyonlarının makrohalkalaşmalarının kapsamlı araştırması yapılmıştır ve benzer sonuçlar elde edilmiştir. Bunun yanısıra C-ucu serbest asit içeren KRNGVIIAGY model peptidi kullanılarak daha büyük *b* iyonlarının davranışı araştırılmış tekli-protonlanmış içsel amino asit kopmalarının yanısıra çifte-protonlanmış amino asit kopmaları da elde edilmiştir. Bu bilgilerden yola çıkılarak yeni bir mekanizma türetilmiştir.

Dedicated to;

the memory of my grandmother Fatma KENAR

TABLE OF CONTENTS

LIST OF FIGURES

Figure **Page**

LIST OF TABLES

Table **Page**

LIST OF ABBREVIATIONS

μL	Microliter
μM	Micromolar
3D	Three-Dimension
Ar	Argon
as-DPD	Asymmetric doubly-protonated dimer
au	Arbitrary unit
B	Magnetic Sector
CAD	Collisional-Activated Dissociation
CI	Chemical Ionization
CID	Collision-Induced Dissociation
Da	Dalton
DC	Direct Current
DFT	Density Functional Theory
E	Electric Sector
ECD	Electron Capture Dissociation
EI	Electron Ionization
EM	Electron Multiplier
ESI	Electrospray Ionization
ETD	Electron Transfer Dissociation
FAB	Fast Atom Bombardment
FD	Field Desorption
FI	Field Ionization
FT-ICR	Fourier Transform-Ion Cyclotron Resonance
GC	Gas Chromatography
H/D	Hydrogen-Deuterium
He	Helium
HPLC	High Performance Liquid Chromatography
Imm	Iminium Ion
IT	Ion-Trap
IT-TOF	Ion-Trap/Time-of-Flight
kDa	Kilo Dalton

kV	Kilovolts
LIT	Linear Ion-Trap
M	Molarity
m/*z*	mass-to-charge ratio
MALDI	Matrix-Assisted Laser Desorption/Ionization
MCP	Microchannel Plate
mg	Milligram
min	Minute
ms	Millisecond
MS	Mass Spectrometry
MS/MS	Tandem Mass Spectrometry
MS^n	Multi-Stage Tandem Mass Spectrometry
N_2	Nitrogen
NCE	Normalized Collision Energy
NIST	National Institute of Standards and Technology
PD	Plasma Desorption
PIC	Pathways in Competition
q	Collision Cell
Q	Quadrupole
QIT	Quadrupole Ion-Trap
RF	Radio Frequency
s-DPD	Symmetric doubly-protonated dimer
TOF	Time-of-Flight
TOF/MS	Time-of-Flight / Mass Spectrometry
UV	Ultraviolet
v	Volume

CHAPTER 1

INTRODUCTION TO MASS SPECTROMETRY

1.1. What is Mass Spectrometry?

Mass spectrometry (MS) is a technique used to separate and detect gas-phase ions qualitatively and quantitatively based on their individual mass-to-charge ratio (*m*/*z*). The idea of mass spectrometry was first suggested by Sir J. J. Thomson[1] in the 1800s. His studies were based on the conductivity of electricity with gases and his studies brought on the discovery of electrons. Thereafter, Thomson and his students separated non-radioactive stable isotopes of neon (neon-20 and neon-22) on photographic plate according to their different parabolic trajectories in the electromagnetic field in 1900s. This experiment is today accepted as the invention of the first mass spectrometer. Nowadays, mass spectrometry can be applied to a wide range of fields such as biotechnology, geology, clinical testing, environmental analysis, pharmaceutical and forensics.

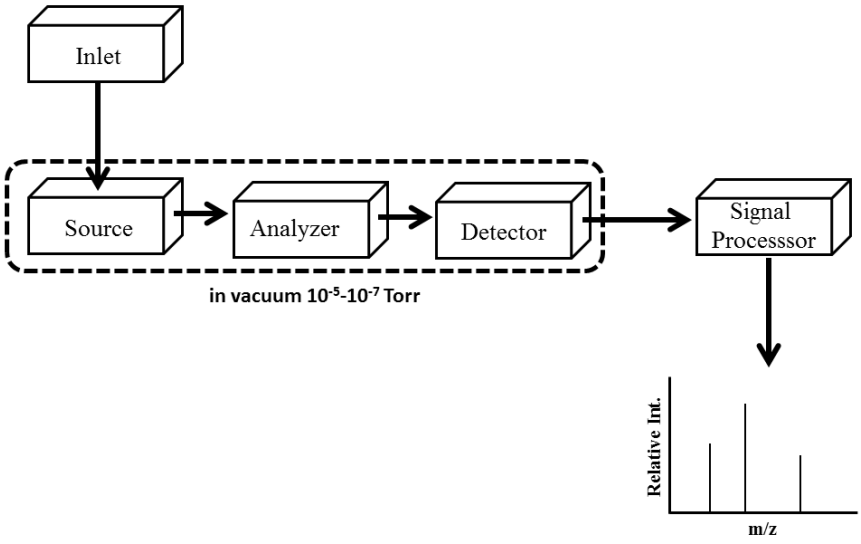

Figure 1.1. Basic components of a mass spectrometer

A mass spectrometer is an analytical instrument which generates gas-phase ions from an analyte and then separates and detects those ions according to their individual mass-to-charge ratios. It consists of three major components: an ionization source, a mass analyzer and an ion detector, as illustrated in Figure 1.1.

Firstly, the sample is introduced into the system through the instrument of a sample inlet which can be HPLC (high performance liquid chromatography), GC (gas chromatography), a syringe, a plate or a probe. The sample is ionized by a source. Then, the positive or negative charged particles are propelled into a mass analyzer and sorted according to their *m*/*z* values by the help of electric or magnetic fields. Following, the ion energy is converted into electrical signals by the detector and transmitted to a computer. Finally, the signals are displayed as a mass spectrum. The whole system is generally operates under vacuum condition (10^{-5}-10^{-7} Torr) for preventing collisions among ions and other gas molecules. In this way, a suitable pressure environment is created ensuring a mean free path of ions large enough to avoid collision.

1.2. Ionization Techniques

The samples are converted to negative or positive ionic species either by losing or gaining of hydrogen (or by losing or gaining electrons) in a gas phase. A variety of ionization techniques are used from past to present such as electron ionization (electron impact, EI)[2], chemical ionization (CI)[3] field ionization/field desorption (FI/FD)[4] plasma desorption (PD)[5] fast atom bombardment (FAB)[6].

The development of soft ionization techniques such as electrospray ionization (ESI)[7], and matrix-assisted laser desorption/ionization (MALDI)[8] is made possible to produce protonated or multiply protonated peptides. The process with MALDI and ESI takes place yield molecules in the gas-phase without fragmentation hence this is why that can be called as soft ionization techniques.

1.2.1. Electrospray Ionization (ESI)

Electrospray ionization (ESI) is a very sensitive ionization technique with certain advantages such as continuous flow operation, wide solvent flow rates, tolerance to different types of solvent, and ability to generate intact multiply charged ions of

fragile chemical and biochemical species. It is also used as an interface HPLC and mass spectrometry. ESI method was first introduced[7a] in 1968. Dole's group electrosprayed the solution of an analyte and electrically charged liquid droplets emerged which generated gas phase ions. However, coupling ESI to MS was introduced by Fenn and co-workers[9] in the mid-1980s. ESI-MS method is substantial for analysis of biomolecules and in the mass range of over 100 kDa can be determined with an accuracy of <0.01 % using this soft ionization method without degradation.

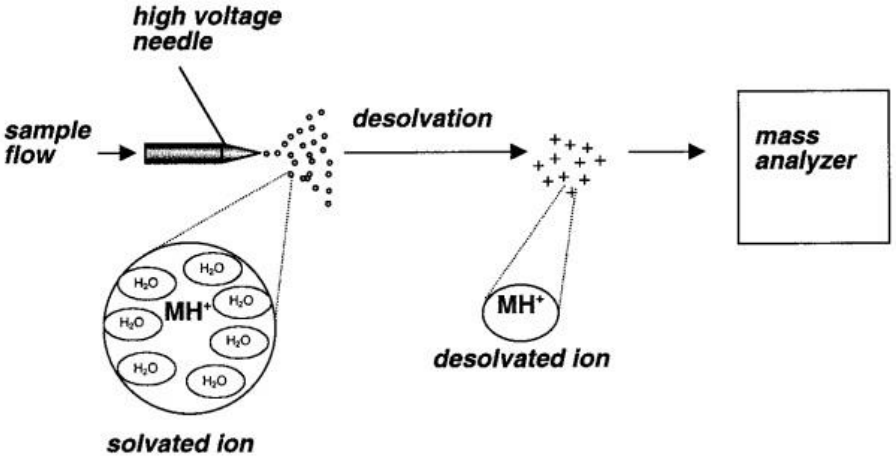

Figure 1.2. Schematic representation of an ESI source[10]

The main principle of ESI is shown in Figure 1.2. The analyte is mixed with a solvent and sprayed from a narrow tube. Charged droplets with the spray transferred into the mass spectrometer sampling orifice with a metal capillary needle influence of electrostatic forces and pressure differentials. A high voltage (3-5 kV) is enforced between capillary and counter electrode to generate a fine aerosol to form "Taylor cone".[11] As the droplets move toward the orifice, the solvent evaporates, resulting in an increased surface charge with helping a flow of drying nitrogen gas. The size of the droplets is reduced and Coulombic forces cause achieving the droplets to Rayleigh limiting charge. Finally, the charged sample ions move towards the mass analyzer.

1.2.2. Matrix Assisted Laser Desorption Ionization (MALDI)

Matrix-assisted laser desorption/ionization, represented as MALDI, was first introduced by two different research groups at the same time in 1988; Karas and Hillenkamp[8a] and Tanaka and co-workers[8b].

This technique has been used primarily to ionize very large biomolecules with masses more than 1000 kDa. The basic feature of MALDI is using a matrix solution such as weak organic acid which is absorbed by ultraviolet (UV) radiation. In this technique, analyte is dissolved in an organic solvent and mixed with matrix solution. The mixture is deposited onto MALDI target plate (stainless steel or gold coated). After the solvent evaporates, a crystalline mixture (sample and matrix) remains on the plate. Subsequently, the target plate is moved into the ion source of the mass spectrometer, and a laser beam is focused on the sample. The laser pulses cause vaporization of the matrix and analyte together from the solid state to the gas-phase. Most of the energy is absorbed by the matrix and no degradation occurs for sample or analyte. Afterward, gas-phase analyte ions are sent to the mass analyzer.

1.3. Mass Analyzers

In a mass spectrometry, the ions are separated according to the individual mass-to-charge (m/z) ratios in a mass analyzer. A mass analyzer enhances the transmission of all ions coming from the ion source and focuses the ions to a single focal point to collect all mass-resolved ions. The charged particles are separated from each other on the basis of momentum, kinetic energy, and velocity. The distinctive features of a mass analyzer are mass range, resolution $(m/\Delta m)$, scan speed, and detection sensitivity.

Magnetic sector, quadrupole (Q), quadrupole ion trap (QIT), time-of-flight (TOF), Fourier transform ion cyclotron resonance (FT-ICR), etc. are the most common analyzer on the market.

1.3.1. Quadrupole (Q)

A quadrupole has four parallel, cylindrical, metal rods fixed time dependent radio frequency (RF) and time independent direct current (DC) potentials to opposite

pairs of electrodes that are connected to each other by means of electrical energy (Figure 1.3). Two rods are positively charged; and two rods are negatively charged, reciprocally. At a certain RF and DC voltages are applied to the rods only ions of specific *m*/*z* value (resonant ions) have stable trajectories and travel into rods to the detector. On the other hand, the remainder of the ions (non-resonant ions) have unstable trajectories are thrown out of the rods so they cannot be detected. By applying continuous RF voltage, a stable trajectory is provided and a full spectrum is observed. For that reason, quadrupoles are used in scanning mode instead of filtering mode.

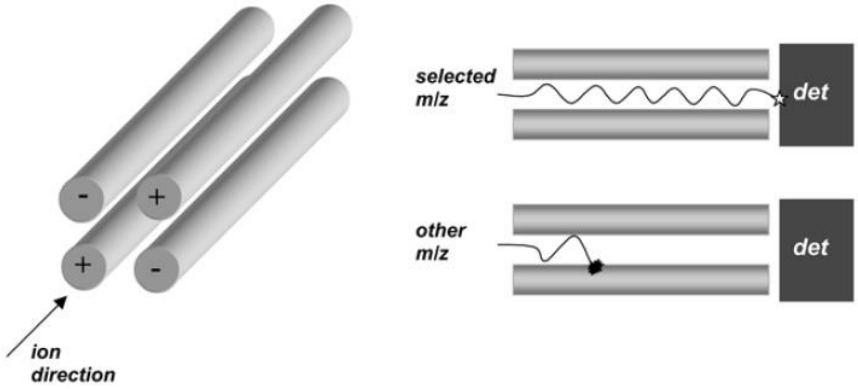

Figure 1.3. Schematic representation of a quadrupole mass analyzer[10]

1.3.2. Ion-Trap (IT)

Ion traps (IT) are a combination of magnetic or electric field that store and direct ions, in a region of a vacuum system or a tube, in time rather than in space. IT mass analyzer was first discovered by Paul and Steinwedel[12] but it was developed by Stafford and co-workers[13] in 1984.

Three dimensional (3D) ion traps[13] which trapping of ions performed by applying RF quadrupole electric field in three dimensions is also named quadrupole ion-trap (QIT). The QIT mass analyzers have linear forms (LIT)[14] in which its working principle is the same as the 3D forms. The QIT is consisted of three electrodes; two end-cap electrodes and a ring electrode, each of have a hyperbolic internal surface to the central cavity. The ring electrode is fitted in between two end-cap electrodes, shown in Figure 1.4.

Firstly, the ions are generated in the ionization source; they are focused on the center of the QIT. The low RF voltage is applied only to the ring electrode and RF voltages create an electrical field since the trap ions within QIT for a period of time. Helium (He) gas (purity >99.9%), is used as damping gas or bath gas, at a pressure of 10^{-3} Torr to the trapping region. It decreases the kinetic energy of the ions. Additionally, using damping gas leads to promote both the mass resolution and sensitivity. With the help of bath gas, all trapped ions are cooled down and move in a complex motion with an oscillation frequency in the cavity of the trap.

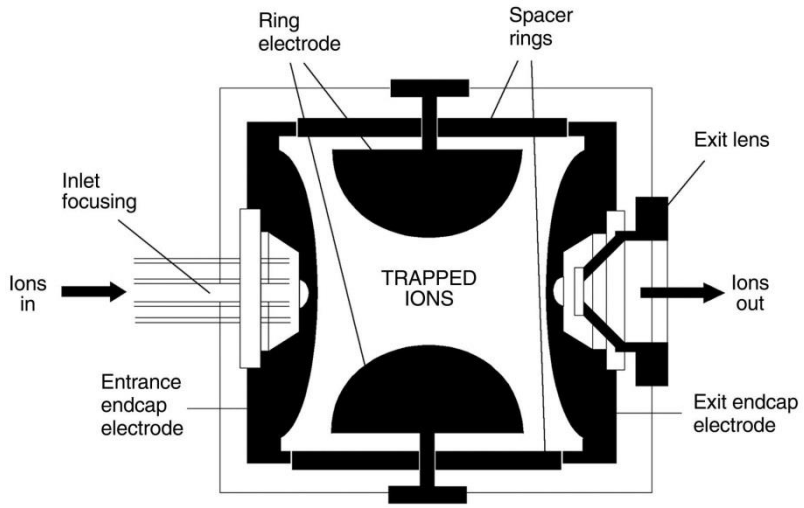

Figure 1.4. Schematic representation of a quadrupole ion trap[10]

The most probably, the most considerable property of ion traps is their amplitude to perform multi-stage tandem mass spectrometry (MS^n) experiments. These experiments provide extensive structural information of the analyte. "*n*" refers to the stage and twelve stages of tandem mass spectrometry have been succeeded[15]. Quadrupole ion traps are worldwide used due to their high sensitivity, high specificity, mechanical simplicity, and capability of MS^n experiments.

1.3.3. Time-of-Flight (TOF)

The theory of time-of-flight (TOF) mass analyzer was firstly described by Stephens[16] in 1946. However, combination of TOF and MS systems was introduced by

Wiley and McLaren[17]. The measurement of velocity of the ions is the basic principle for TOF mass analyzer. The ions are separated according to their different velocities. The magnetic or electric fields do not act (field-free) on the ions during ions flight in TOF tube. The ions are accelerated towards the detector with the same kinetic energy which creates potential differences between acceleration electrodes and entry grid. The heavier ions reach the detector later because of their lower velocity whereas lighter ions reach the detector faster due to their higher velocity. The duration of flight of ions between the source and the detector are measured, and ions are quantified. Moreover, all formed ions will reach the detector one by one. The principle of the mass separation by a TOF mass analyzer is illustrated in Figure 1.5.

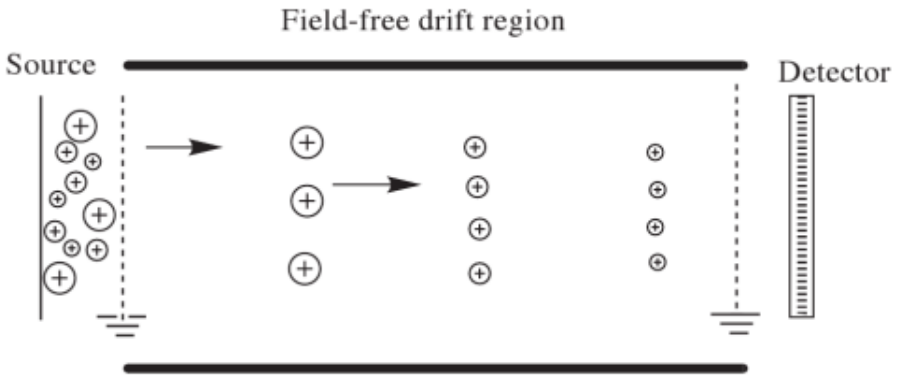

Figure 1.5. Principle of the mass separation by TOF[18]

A primary requirement in the function of a TOF-MS is that all ions enter the flight tube implicitly at the same time. Creating ions in short explosions performs this condition. In this respect, TOF instruments are well matched to plasma desorption (PD) and MALDI ion sources.

1.3.4. Fourier Transform Ion Cyclotron Resonance (FT-ICR)

The ion cyclotron resonance technique was discovered firstly by Hipple and co-worker[19] and Fourier transform ion cyclotron resonance (FT-ICR) mass spectrometry was introduced in the early 1970s by Marshall and Comisarow[20]. Due to its incomparable high resolution and detection capabilities FT-MS has a worldwide acceptability as an analytical tool for analysis of biomolecules.

The technique is based on the principle of ion cyclotron resonance (ICR), in which ionization, mass analysis, and detection occur in the same region, usually in a cubic or cylindrical cell that is placed in a strong magnetic field. The fundamental of mass analysis in ICR is that an ion when stayed in a magnetic field will move at a frequency that is characteristic of its *m*/*z* value. The ions move in circular orbit in a plane perpendicular to the field. An ICR cell has three different plates which are located oppositely, illustrated in Figure 1.6.

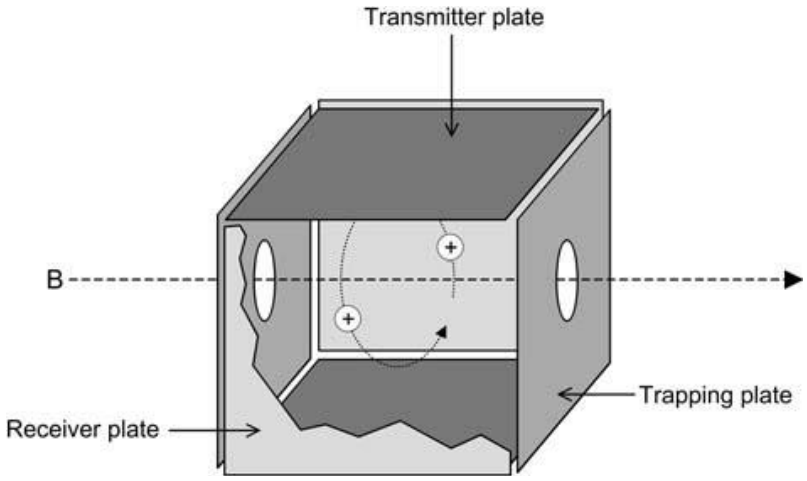

Figure 1.6. FT-ICR mass analyzer[21]

A broadband excitation pulse is applied to the transmitter plates of the cell and ions that have different *m*/*z* values absorb energy from this pulse signal and are forced to move in phase-coherent packets of larger orbits. They transmit a complex RF signal that contains specific frequency for each ion whiles these ions coherently moving around to the receiver plate. This induced signal is converted a time-domain free-ion decay signal. And then, this signal is converted into a frequency-domain signal to derive the simultaneous detection of all ions with a wide mass range.

1.3.5. Hybrid Mass Analyzer

Combination of two or more mass analyzers together is called hybrid or tandem mass analyzer system. Higher sensitivity and mass accuracy can be obtained in one instrument. Analyzer combination can be designed as EBE[22], EBEB[23], BEqQ[24], IT-TOF[25], Q-TOF[26], QqQ[27] etc. Hybrid mass spectrometers are invented where capital

letters of B, E, q, and Q indicates that a magnetic sector, an electric sector, a collision cell, and a mass filter, respectively.

1.4. Ion Detectors

The last part of a mass spectrometer is a detector. A detector must have some features such as a high amplification, a high stability, a large dynamic range, a low cost and a low or no noise. The most common used detectors are Faraday cup, electron multiplier (EP), and microchannel plate (MCP).

1.4.1. Faraday Cup

Faraday cup consists of a metal cup with a small orifice. When the ions hit the walls of the metal cup, an ion current is produced and the ions gain small net charge while they are neutralized. Thus, the induced current is amplified and detected.

1.4.2. Electron Multiplier (EM)

The electron multiplier (EM) has a range of dynodes. These dynodes increase potentials with gaining speed to ions. Secondary electrons are emitted of the first dynode, and they are multiplied in a cascade by the next dynodes until collected by a metal anode and detected (see Figure 1.7).

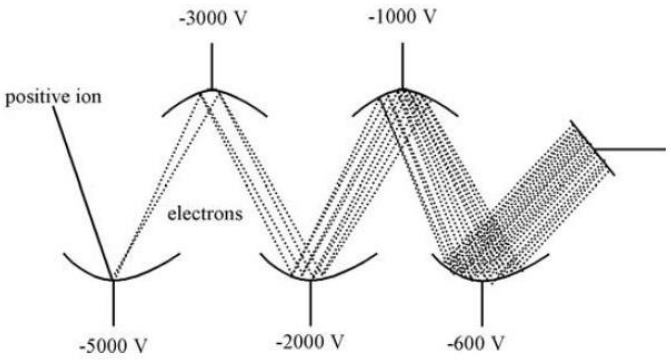

Figure 1.7. Electron multiplier ion detector[18]

1.4.3. Microchannel Plate (MCP)

A microchannel plate (MCP) detector is closely related to an EM as increase velocity of ions by multiplication of electrons via secondary emission[28]. It has huge number of independent channels. Each channel is assumed as a continuous-dynode electron multiplier which supplies higher spatial and temporal resolution. In consequence of collision of secondary electrons and channel surface, much more secondary electrons are obtained and after repetition of this process several times, thousands of electrons are emitted to be detected.

CHAPTER 2

FRAGMENTATION REACTION MECHANISMS OF PROTONATED PEPTIDES IN THE GAS PHASE

2.1. Amino Acids and Peptides

Amino acids are biological organic molecules consist of an amine group, a carboxylic acid functional group, and a specific side chain group (R). Twenty naturally occurring amino acids are listed in Table 2.1. Amino acids are constituent of the proteins. Proteins can be produced from amino acids by way of condensation reaction and the new bond between CO and NH linkage is called peptide bond, shown in Figure 2.1.

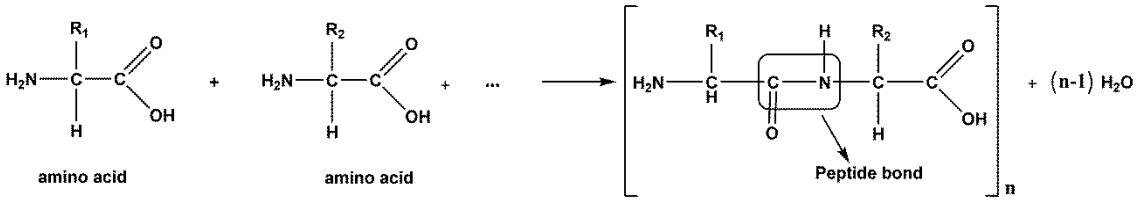

Figure 2.1. Peptide bond formation

Proteins are huge biological molecules and they have biological importance in cell, such as storage, repairing, structural support, cellular signaling, energy, movement and defense mechanisms. Defining the amino acid sequence of proteins has crucial importance in system biology because the proteins can be considered as biomarkers in disease diagnosis. Hence, tandem mass spectrometry is more powerful technique in peptide sequencing and protein identification with collision induced dissociation.

Table 2.1. Common amino acid residues

Name	3-letter Symbol	1-letter Symbol	Monoisotopic Mass (Da)	Immonium Ion Mass (Da)
Glycine	Gly	G	57.021	30
Alanine	Ala	A	71.037	44
Serine	Ser	S	87.032	60
Proline	Pro	P	97.053	70
Valine	Val	V	99.068	72
Threonine	Thr	T	101.048	74
Cysteine	Cys	C	103.009	76
Isoleucine	Ile	I	113.084	86
Leucine	Leu	L	113.084	86
Aspartic Acid	Asp	D	114.027	88
Asparagine	Asn	N	114.043	87
Glutamine	Gln	Q	128.059	101
Lysine	Lys	K	128.095	101
Glutamic Acid	Glu	E	129.043	102
Methionine	Met	M	131.04	104
Histidine	His	H	137.059	110
Phenylalanine	Phe	F	147.068	120
Arginine	Arg	R	156.101	129
Tyrosine	Tyr	Y	163.063	136
Tryptophan	Trp	W	186.079	159

2.2. Tandem Mass Spectrometry (MS/MS) and Collision-Induced Dissociation (CID)

Tandem MS is a world-wide known technique in protein chemistry for more reliable information.

A typical tandem mass spectrometer consists of at least two stages of mass analyses. Mass selection, mass fragmentation and mass analysis are the three fundamental stages of a tandem MS, shown in Figure 2.2.

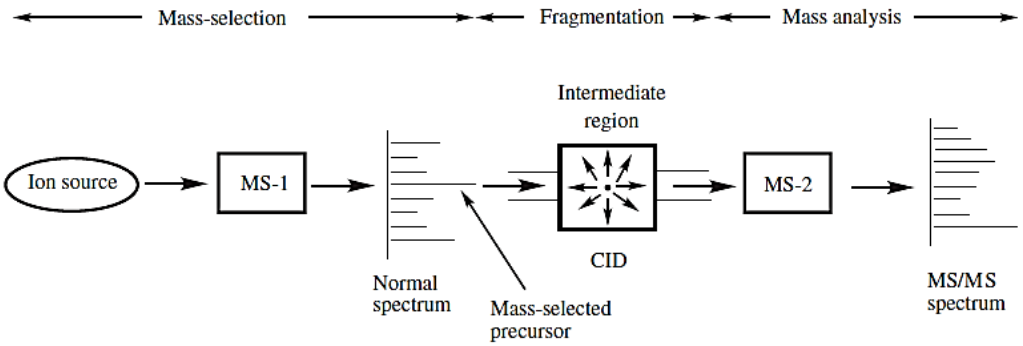

Figure 2.2. Basic principles of TOF/MS[18]

The first analyzer (MS-1) can be used to select the ion of interest and then selected ion, such as *parent* or *precursor ion*, undergoes fragmentation via collision with inert gas (e.g. He, Ar, Xe or N_2) in the collision cell. The second mass analyzer (MS-2) can be used to obtain *daughter ions* which generated from parent or precursor ion after collision. Fragmentation of parent or precursor ion via collision with inert gas is known as collision induced dissociation (CID) or collisional activated dissociation (CAD).

Achieving the correct and reliable peptide sequencing plays a crucial role for proteomic studies. Therefore, development of tandem MS technique to understand gas phase fragmentation reaction mechanism pathway of peptides will bring breakthrough for this area.

2.3. Peptide Fragmentation Chemistry

Elucidating of peptide sequencing and protein identification are very popular research areas in the world and understanding the gas-phase fragmentation reaction mechanism of peptides is important to sequence of unknown peptides or proteins correctly.

2.3.1. Mobile Proton Model

There are several mechanisms to explore the fragmentation reaction mechanism of protonated peptides such as mobile proton model[29], pathways in competition, charge-directed etc. under low energy CID conditions[30]. The captured proton is usually located

on N-terminal amino group or amide carbonyl oxygen or side chain groups of Arg (R), Lys (K), and His (H) for singly charged ion[31]. Under the CID condition proton prefers the thermodynamically less stable site of the peptide backbone and further bond breaking occur. In generally, when the CO-NH amide bond is broken during the CID *b* and *y* fragment ions can be obtained.

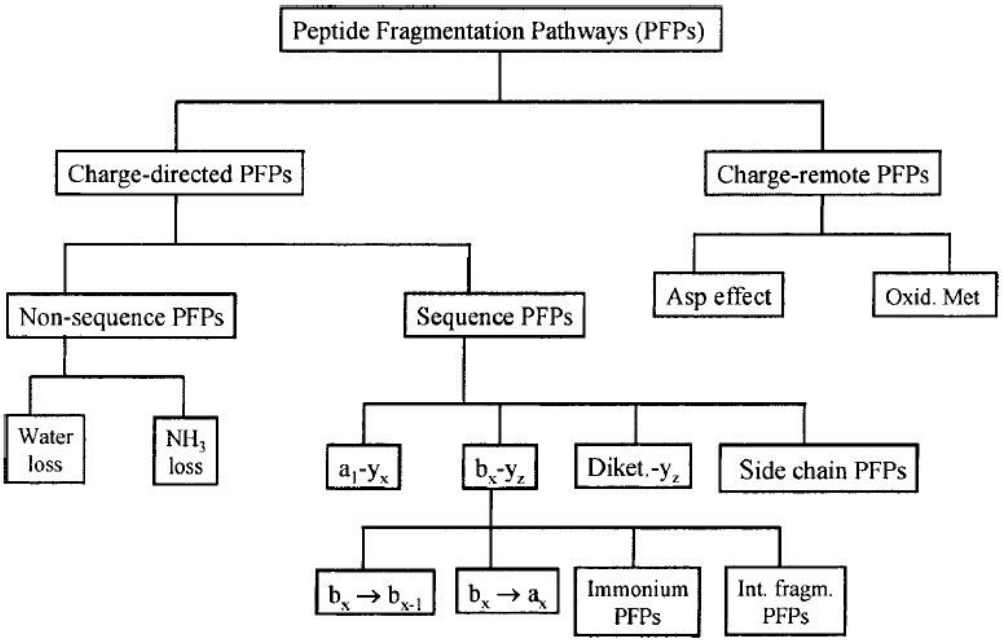

Figure 2.3. Peptide fragmentation pathways[32]

Pathways in competition (PIC) mechanism, shown in Figure 2.3, were proposed by Paizs and Suhai[32] in 2005. They have developed a new pathway in order to generate more understanding course of gas-phase fragmentation mechanisms.

2.3.2. Peptide Fragmentation Nomenclature

Nomenclature of peptide fragmentation[33] is improved by Biemann in 1988 and is shown in Figure 2.4.

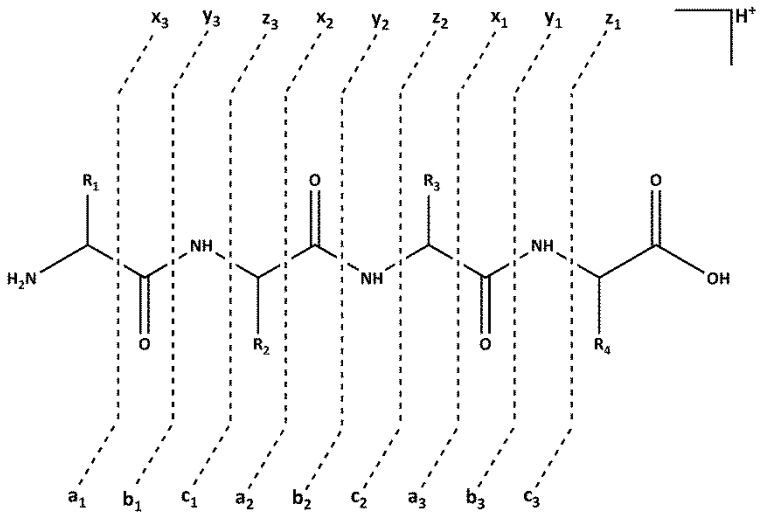

Figure 2.4. The nomenclature of peptide fragment ions

During the peptide fragmentation via CID, if the charge remains on N-terminal during the bond breaking, the ion formed is called *a*, *b* or *c;* if the charge remains on C-terminal, the ion formed during the bond breaking it is called *x*, *y* or *z*. Mainly, *b*, *y* and *a* ions can be obtained for peptide fragmentation under the low energy CID conditions. Under the high energy CID conditions, ETD (electron transfer dissociation) and ECD (electron capture dissociation) techniques, predominantly *c* and *z* ions are obtained through the cleavage of N-C_α bond[34].

The CO elimination from *b* ion gives *a* ion fragment. Additionally, water and ammonia cleavages are detected from fragment ions and symbol "^{o}" emphasizes water-loss and symbol "*" emphasizes ammonia-loss from the indicated ions.

Internal amino acids fragments and iminium ions of amino acids are also obtained in the MS/MS spectra. Iminium ions ($RCH=NH_2^+$) are distinction property of amino acids present in the peptide.

2.3.3. Structures of *b* Ion

Since generally *b* ions give the direct information about the peptide sequence, variety of studies has been established about structure of *b* ions[32, 35] . Four different structures of *b* ions were proposed, namely acylium ion, diketopiperazine ion, oxazolone ion, and macrocyclic ion in the literature.

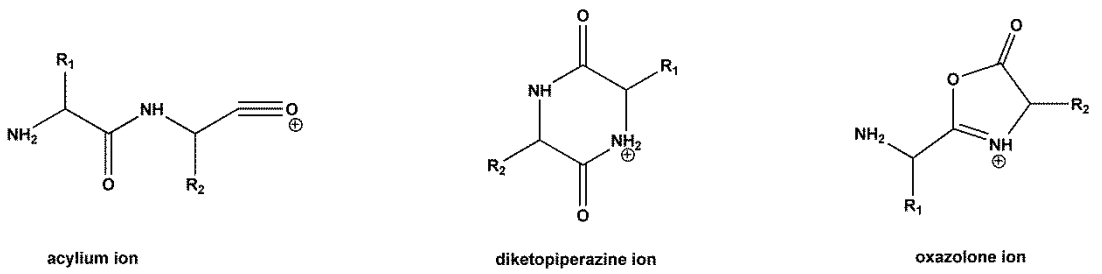

Figure 2.5. Possible structures of b_2^+ ion

The first representation belongs to an acylium ion[33] for a singly-charged b_2 ion. This ion is not a thermodynamically stable structure and it loses CO immediately and converted into a stable iminium ion. Six-membered ring diketopiperazine structure[36] is another form of b_2^+ ions which is formed by nucleophilic attack of N-terminal nitrogen atom on the second carbonyl carbon of the protonated amide bond. The possible structures of b_2^+ ions are shown in Figure 2.5.

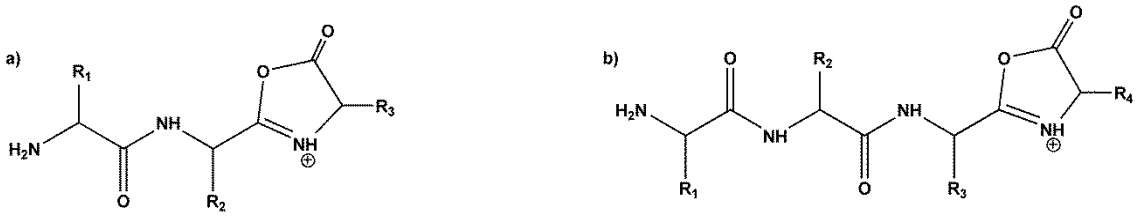

Figure 2.6. Possible structures of a) b_3^+ b) b_4^+ ions

Subsequent elaborative studies proved that small b_n (n=2-4) ions give stable five-membered oxazolone ring structure[35c, 35d], illustrated in Figure 2.6. The formation of oxazolone structure is formed via nucleophilic attack of the N-terminal adjacent backbone carbonyl oxygen to the next C-terminal carbonyl carbon of the protonated amide. Most recently, another structure have been proposed for the bigger b (b_n; n≥5) ions, named macrocyclic structure[37] (Figure 2.7). Macrocyclization is taken place via attack of N-terminal amine group to the carbonyl carbon of the oxazolone ring which is resided at the C-terminal of the peptide, illustrated in Figure 2.8. On the other hand, it should be noted that b_4^+ ions have 40 % oxazolone and 60 % macrocyclic ion structure.

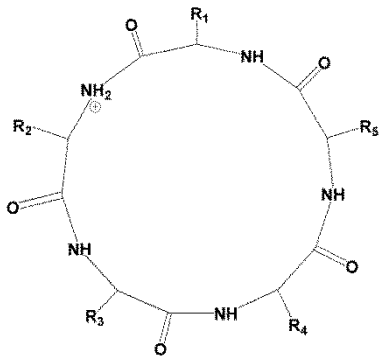

Figure 2.7. Possible structure of b_5^+ ion

The opening reaction of macrocyclic structure causes *non-direct* amino acid fragmentation which is also called *sequence scrambling*. Non-direct sequence ion eliminations are demonstrated that sequence scrambling can only be observed with formation of macrocyclic *b* ions.

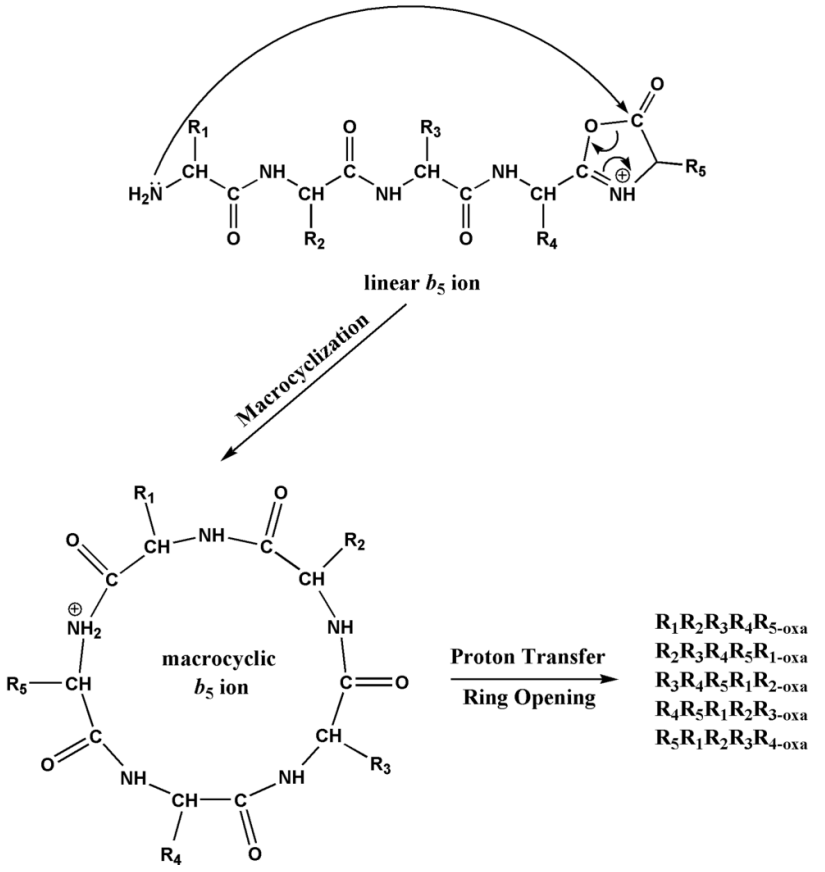

Figure 2.8. Proposed mechanisms for the formation of macrocyclic b_5^+ ion

2.3.4. Doubly-Charged Studies in Mass Spectrometry

With the implementation of the soft ionization techniques of ESI and MALDI, tandem MS with CID of protonated and multiply-protonated peptides have become commonly used technique for emphasizing of amino acid sequence of peptides. Most of the gas-phase fragmentation studies are focused on singly-protonated peptides. On the other hand, there were limiting studies for doubly-protonated peptides.

In the earlier work, the fragmentation pathways of doubly-protonated peptides were researched[38]. Mechanisms of some tryptic peptides and importance of location and number of basic amino acid residues for fragmentation of multiply-charged peptides were investigated under low CID conditions. Besides, redundancy of *b* and *y* ions in the multiply-charged ions spectra was showed.

Another study has been examined the doubly-charged peptides using quadrupole ion trap mass spectrometry[39]. Internal amino acid eliminations were labeled based on head-to-tail cyclization of singly-charged *b* ions.

Statistical characterization of more than one thousand doubly-charged tryptic peptides were examined by ion trap tandem MS which median length were 15 residues[40]. The peptides were investigated according to the link between peak intensity and fragment ions, effects of adjacent amino acid on amide bond cleavage, and relationship of types of amino acid and neutral loss fragments.

In 2008, huge number of doubly-protonated tryptic peptides was divided into two classes according to their *b*/*y* complementary fragments[41].

By using tandem MS, H/D (hydrogen/deuterium) exchange, and density functional calculations methods the structure of b_2 ions of doubly-protonated peptides (YIGSR, YGGFLR, and YIYGSFK) were investigated[42].

In the another research, $(Ala)_xHis$ (x=5, 6, 7, 8, and 10) peptide series were investigated the effects of chain length on the formation of b_2 and its complementary ion y_{n-2} from doubly-charged peptides. Researchers suggested that peptide chain length plays a substantial role in the bifurcating behavior of fragmentation of doubly-protonated peptides[43].

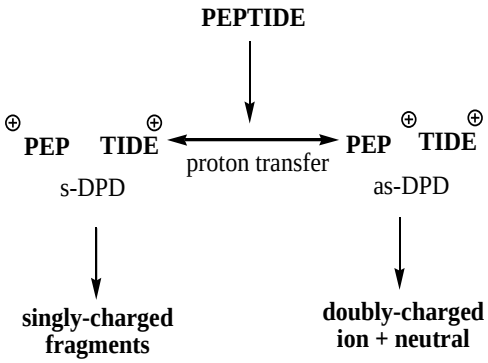

Figure 2.9. Routes of fragmentation of doubly-protonated peptides

The research that has been done in 2009 was the first known study related to the doubly-protonated *b* ions[44]. In this study, it was claimed that doubly-protonated peptides may fragment with two different ways: by charge-separation reactions to generate two singly-charged fragments or as a doubly-protonated fragment and a neutral form, illustrated in Figure 2.9 where "as-DPD" refers to asymmetric doubly-protonated dimers and "s-DPD" symmetric doubly-protonated dimers.

From this point of view, Proline (Pro) included tryptic heptapeptides were studied with the doubly-protonated form[45]. In this study, it was suggested that tendency of asymmetric cleavage decreases while Pro residue closers to the Arg residue. Hence, position of the basic residues affects the pathways of doubly-protonated fragmentation.

The effect of the amino acid residue was investigated using Ala-Ala-Xaa-Ala-Ala-Ala-Arg peptide series (Xaa= Ala (A), Ser (S), Val (V), Thr (T), Ile (I), Phe (F), Tyr (Y), Sar, Met (M), Trp (W), Pro (P), and Gln (Q))[46]. The results showed that symmetric and asymmetric cleavage largely independent of the type of the Xaa residue.

Several sized doubly-charged *b* ions from any tachykinin peptides were investigated performing CAD and ECD and it was suggested that a *b* ion may be acquired as a mixture of various form according to the length and side chain groups of peptide[47].

Another research group have been developed a rule using NIST (The National Institute of Standards and Technology) peptides which showed the peaks had *m*/*z* of y_{n-1}+10 and y_{n-1}+11 (n =number of amino acid residue) via tandem mass spectra. In addition, there have been studies of CID of doubly-charged *a* ($[a_2+H]^{2+}$ and $[a_3+H]^{2+}$) ions using Density Functional Theory (DFT) calculations[48].

2.4. Aim of the Thesis

The elucidation of amino acid sequence of peptides is a substantial issue in order to understand the peptide fragmentation pathways. Especially behaviors of *b* ions play significant role for finding peptide sequence correctly. In the last two decades, many reports have been appeared in the literature for the gas-phase fragmentation reactions of doubly-protonated ions. However, there are very limited researches about doubly-protonated *b* ions.

In here, we aimed to investigate the fragmentation reactions of doubly-protonated *b* ions derived from basic amino acid containing model peptides. Histidine is selected as a basic amino acid residue which can hold one proton on its side-chain (imidazole group), to investigate doubly-charged macrocyclic behavior of b_7^{2+} ions. Two sets of model peptides were used, for this purpose. The resultant mass spectra are examined in terms of internal amino acid eliminations which is the consequence of macrocyclization reaction of doubly-protonated *b* ions. Different from those samples variety of C-terminal free acid peptides were examined and aimed to find macrocyclization reactions of doubly-protonated larger b_8 and b_9 ions.

CHAPTER 3

EXPERIMENTAL

3.1. Materials

Two sets of C-terminal amidated model peptides HYAGFLV-NH_2, YHAGFLV-NH_2, YAHGFLV-NH_2, YAGHFLV-NH_2, YAGFHLV-NH_2, YAGFLHV-NH_2, YAGFLVH-NH_2 and HAAAAAA-NH_2, AHAAAAA-NH_2, AAHAAAA-NH_2, AAAHAAA-NH_2, AAAAHAA-NH_2, AAAAAHA-NH_2, AAAAAAH-NH_2 and one set of C-terminal free acid model peptides SVEHAGVIL-OH, SHIGDAVVI-OH, EHAGVISVL-OH, GRIDKPILK-OH and KRNGVIIAGY-OH were purchased from GL Biochem Ltd. (Shanghai, China) and used without any purification step. HPLC-grade methanol and formic acid were obtained by Merck (Darmstadt, Germany) and ultrapure grade water (18.2 MΩ) was used (Arium 611 UV, Sartorius AG, Gottingen, Germany) throughout the study. A 1-1.5 mg of each solid peptide sample was dissolved in 1:1 (v/v) CH_3OH:H_2O to prepare stock solutions with a concentration of 10^{-2} or 10^{-4} M. Peptide samples at micromolar concentration were prepared by diluting 1:1 (v/v) CH_3OH:H_2O and 1% formic acid.

3.2. Mass Spectrometry

All multistage mass spectrometry (MS^n) experiments were carried out an LTQ-XL linear ion-trap mass spectrometer (Thermo Finnigan, San Jose, CA, USA) equipped with an ESI source. Before each experiment, the instrument was calibrated with the company's calibration mixture (Calmix: caffeine, MRFA, and Ultramak). All the experimental settings (voltage, lens, multipole, offset etc.) were optimized for maximum $[M+2H]^{2+}$ ion peak using the tuning routine within the LTQ tune program. A 100 μM peptide solution was prepared in 50:50:1 (v/v/v) CH_3OH/H_2O/HCOOH and infused into the ion source with an incorporated syringe pump at a flow rate of 5 μL/min. Ion spray voltage was kept at + 5.00 kV and nitrogen gas was used as a 10-10-1 or 8-8-0 arbitrary unit (au) as a sheath gas, auxiliary gas, and sweep gas, respectively.

Helium gas was used as a bath/buffer gas (cooler gas) to improve trapping efficiency. The capillary temperature was maintained at 325 °C. Normalized collision energy (NCE) was set at between 16-23 % with activation (*q*) of 0.250, and activation time of 30 ms was applied at each CID stage. The isolation width (*m/z*) for precursor and daughter ions was set at between 1.0-2.5 for C-terminal amidated YAGFLV and whole C-terminal free acid model peptide series meanwhile 1.0-1.8 for C-terminal amidated AAAAAA model peptide series MS acquisitions. Moreover, nearly 400 scans were averaged with a scan rate of 1 employed.

CHAPTER 4

RESULTS AND DISCUSSIONS

4.1. Introduction

To understanding gas-phase fragmentation behavior of *b* ions have vital importance in protein chemistry. Having looked at the literature, tryptic digestion method is a very common technique to obtain peptides from proteins. Trypsin enzyme is a specific enzyme which cut the proteins at a specific point generating C-terminal Arg (R) and Lys (K) positioned peptides. These amino acids are very basic and available to be multiply-protonated.

On the other hand, His (H) is the third most basic amino acid existed in nature. There have been several studies about gas-phase fragmentation behavior of His containing peptides. An analysis doing 505 different tryptic peptides showed that His effects the enhancement of cleavage in doubly-protonated tryptic peptides as an internal amino acid[49]. And also, it is demonstrated that proton affinity takes an important place in determining the intensities of fragment ions. A mechanistic study investigated that His behaves in different ways and generates a *b* ion form unlike oxazolone and acylium ion during dissociation of doubly-protonated peptides[50]. Based upon these researches His residue was used for creating doubly-charged b_7 ion. His residue was positioned in YAGFLV-NH_2 peptide series, because of common usage of it in our research area, and AAAAAA-NH_2 series, because of less reactive feature of Ala residue, from N-terminal to C-terminal. Moreover, macrocyclic behavior of doubly-charged, larger *b* ions (b_8^{2+} and b_9^{2+}) was examined. For this purpose, some peptides including several basic amino acids were synthesized which is compatible with a cell line[51].

All in all, in our study CID of MS^3 behavior of fragment b_n (n =7-9) ions in doubly-protonated peptides were investigated. The results were explained in following sections in detail.

4.2. Investigation of Macrocyclic Behavior of Doubly-Protonated b_7 Ions

The formation of non-direct sequence ions in the MS/MS spectra of doubly-protonated *b* ion can be accepted as an evidence for macrocyclization reaction. In this part of thesis, to investigate macrocyclic behavior of b_7^{2+} ion (MS/MS/MS spectra) upon CID is aimed. The YAGFLV-NH_2 peptide sequence motif was used because the fragmentation characteristics of this sequence have been well studied from our group. Besides, AAAAAA-NH_2 peptide series were used to compare similarities and differences of macrocyclic behavior of His-containing residues between C-terminal amidated YAGFLV and AAAAAA series.

4.2.1. His Residue Containing YAGFLV-NH_2 Peptide Series

Initially, His residue was positioned at the N-terminal of YAGFLV-NH_2 heptapeptides. The CID mass spectrum of the b_7^{2+} (*m*/*z* 394.5) ions was recorded via low energy CID-MS^3 $[M+2H]^{2+} \rightarrow b_7^{2+}$ consecutive experiments (Figure 4.1). Besides, doubly-protonated direct sequence ions such as b_7^* (*m*/*z* 386.0), a_7^{2+} (*m*/*z* 380.5), and b_6^{2+} (*m*/*z* 345.0) and also singly-protonated signals were obtained. These signals indicated that internal eliminations sourced from b_7^{2+} ion namely; $[b_7^{2+}\text{-A}]^+$ (*m*/*z* 717.0), $[b_7^{2+}\text{-V}]^+$ (*m*/*z* 689.0), $[b_7^{2+}\text{-L}]^+$ (*m*/*z* 675.0), $[b_7^{2+}\text{-H}]^+$ (*m*/*z* 651.0), $[b_7^{2+}\text{-F}]^+$ (*m*/*z* 641.0), and $[b_7^{2+}\text{-Y}]^+$ (*m*/*z* 625.0). Moreover, coupled amino acid eliminations and their singly-protonated fragments were observed which are $[b_7^{2+}\text{-VL}]^+$ (*m*/*z* 576.0), $[b_7^{2+}\text{-YA}]^+$ (*m*/*z* 554.0), $[YA]^+$ (*m*/*z* 235.0), and $[VL]^+$ (*m*/*z* 213.0). Additionally, *m*/*z* 136 and *m*/*z* 120 signals were obtained which represent iminium ion of Tyrosine (Y_{imm}) and iminium ion of Phenylalanine (F_{imm}), respectively.

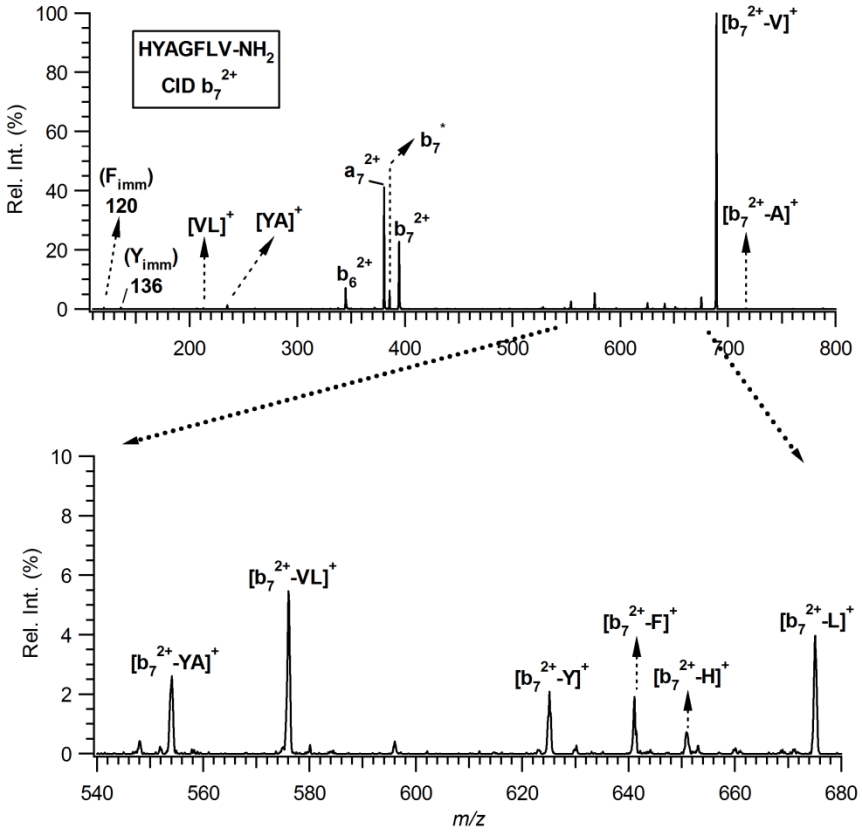

Figure 4.1. CID mass spectra of HYAGFLV-NH_2

When His residue was positioned as the second amino acid counting from N-terminus singly-protonated internal eliminations were obtained, again (Figure 4.2). Besides, doubly-protonated signals such as, a_7^{2+} (*m*/*z* 380.5) and b_6^{2+} (*m*/*z* 345.0), the singly-protonated signals were obtained. These signals indicated that internal eliminations sourced from b_7^{2+} ion namely; $[b_7^{2+}\text{-A}]^+$ (*m*/*z* 717.0), $[b_7^{2+}\text{-V}]^+$ (*m*/*z* 689.0), $[b_7^{2+}\text{-L}]^+$ (*m*/*z* 675.0), $[b_7^{2+}\text{-F}]^+$ (*m*/*z* 641.0), and $[b_7^{2+}\text{-Y}]^+$ (*m*/*z* 625.0). Moreover, coupled amino acid eliminations were observed which are $[b_7^{2+}\text{-FG}]^+$ (*m*/*z* 584.0), $[b_7^{2+}\text{-VL}]^+$ (*m*/*z* 576.0), $[b_7^{2+}\text{-LF}]^+$ (*m*/*z* 528.0), $[b_7^{2+}\text{-YV}]^+$ (*m*/*z* 526.0), $[b_7^{2+}\text{-YH}]^+$ (*m*/*z* 488.0). And also, a triple amino acid elimination namely $[b_7^{2+}\text{-FGA}]^+$ (*m*/*z* 513.0) was obtained from the MS^3 CID of YHAGFLV-NH_2 peptide. Additionally, singly-protonated fragment were achieved such as $[\text{YH}]^+$ (*m*/*z* 301.0), $[\text{FGA}]^+$ (*m*/*z* 276.0), $[\text{VL}]^+$ (*m*/*z* 213.0). With all that, *m*/*z* 136 signal was observed which represent iminium ion of Tyrosine (Y_{imm}).

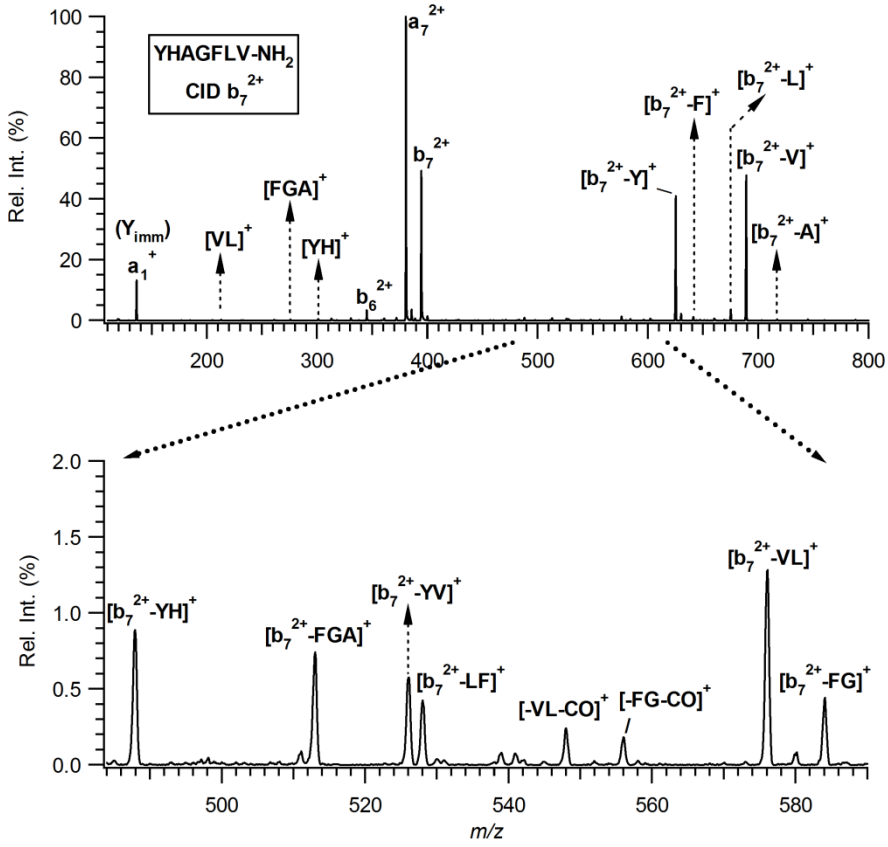

Figure 4.2. CID mass spectra of YHAGFLV-NH_2

His residue was positioned as a third amino acid and its mass spectra was recorded (Figure 4.3).

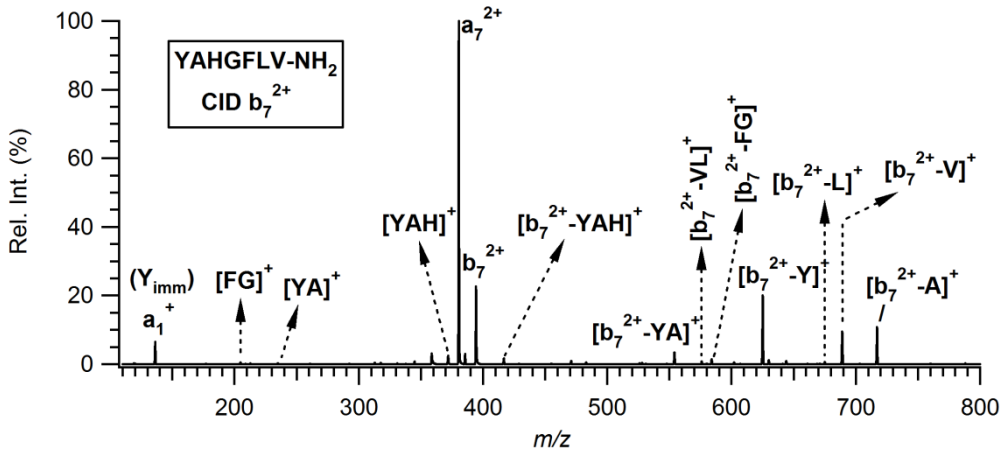

Figure 4.3. CID mass spectra of YAHGFLV-NH_2

The peak at *m*/*z* 380.5 refers to doubly-protonated a_7 ion which is CO elimination from b_7^{2+} ion. It was continued to seemed that the singly-protonated internal amino acid eliminations such as $[b_7^{2+}\text{-A}]^+$ (*m*/*z* 717.0), $[b_7^{2+}\text{-V}]^+$ (*m*/*z* 689.0), $[b_7^{2+}\text{-L}]^+$ (*m*/*z* 675.0), and $[b_7^{2+}\text{-Y}]^+$ (*m*/*z* 625.0). Besides, coupled and triple amino acid eliminations were observed which are $[b_7^{2+}\text{-FG}]^+$ (*m*/*z* 584.0), $[b_7^{2+}\text{-VL}]^+$ (*m*/*z* 576.0), $[b_7^{2+}\text{-YA}]^+$ (*m*/*z* 554.0), and $[b_7^{2+}\text{-YAH}]^+$ (*m*/*z* 417.0). Moreover, singly-protonated fragment were obtained such as $[\text{YAH}]^+$ (*m*/*z* 372.0), $[\text{YA}]^+$ (*m*/*z* 235.0), $[\text{FG}]^+$ (*m*/*z* 205.0). With all that, *m*/*z* 136 signal represented iminium ion of Tyrosine (Y_{imm}).

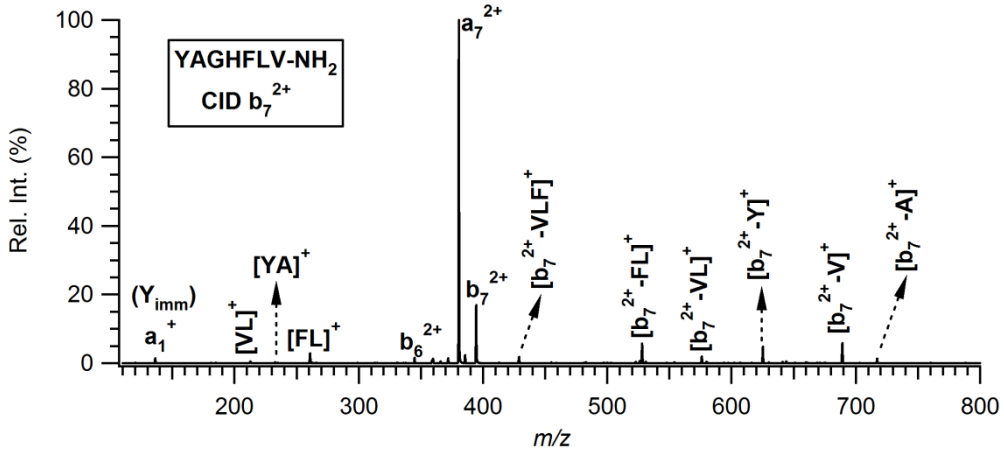

Figure 4.4. CID mass spectra of YAGHFLV-NH_2

The CID MS/MS/MS spectrum of middle positioned His in YAGFLV-NH_2 peptide series still indicated singly-protonated single, double and triple amino acid eliminations namely; $[b_7^{2+}\text{-A}]^+$ (*m*/*z* 717.0), $[b_7^{2+}\text{-V}]^+$ (*m*/*z* 689.0), $[b_7^{2+}\text{-Y}]^+$ (*m*/*z* 625.0), $[b_7^{2+}\text{-VL}]^+$ (*m*/*z* 576.0), $[b_7^{2+}\text{-FL}]^+$ (*m*/*z* 528.0), and $[b_7^{2+}\text{-FLV}]^+$ (*m*/*z* 429.0). Meanwhile, $[\text{FL}]^+$ (*m*/*z* 261.0), $[\text{YA}]^+$ (*m*/*z* 235.0), $[\text{VL}]^+$ (*m*/*z* 213.0) and Y_{imm} (*m*/*z* 136) ions were observed near the doubly-protonated a_7 and b_6 ions which *m*/*z* values are 380.5 and 345.0, respectively (Figure 4.4).

When the His residue at the fifth position counting from N-terminus singly-protonated single and couple amino acids sequences were observed coming from doubly-protonated b_7 ion fragmentation (Figure 4.5).

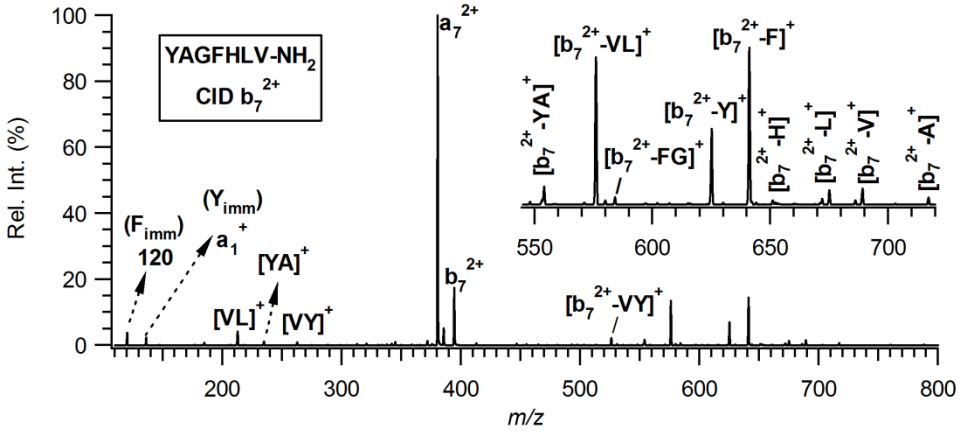

Figure 4.5. CID mass spectra of YAGFHLV-NH_2

In the CID mass spectra of YAGFHLV-NH_2 $[b_7^{2+}\text{-A}]^+$ (*m*/*z* 717.0), $[b_7^{2+}\text{-V}]^+$ (*m*/*z* 689.0), $[b_7^{2+}\text{-L}]^+$ (*m*/*z* 675.0), $[b_7^{2+}\text{-H}]^+$ (*m*/*z* 651.0), $[b_7^{2+}\text{-F}]^+$ (*m*/*z* 641.0), $[b_7^{2+}\text{-Y}]^+$ (*m*/*z* 625.0), $[b_7^{2+}\text{-FG}]^+$ (*m*/*z* 584.0), $[b_7^{2+}\text{-VL}]^+$ (*m*/*z* 576.0), $[b_7^{2+}\text{-YA}]^+$ (*m*/*z* 554.0), $[b_7^{2+}\text{-VY}]^+$ (*m*/*z* 526.0), $[\text{VY}]^+$ (*m*/*z* 263.0), $[\text{YA}]^+$ (*m*/*z* 235.0), $[\text{VL}]^+$ (*m*/*z* 213.0), Y_{imm} (*m*/*z* 136.0), and F_{imm} (*m*/*z* 120.0) signals were recorded.

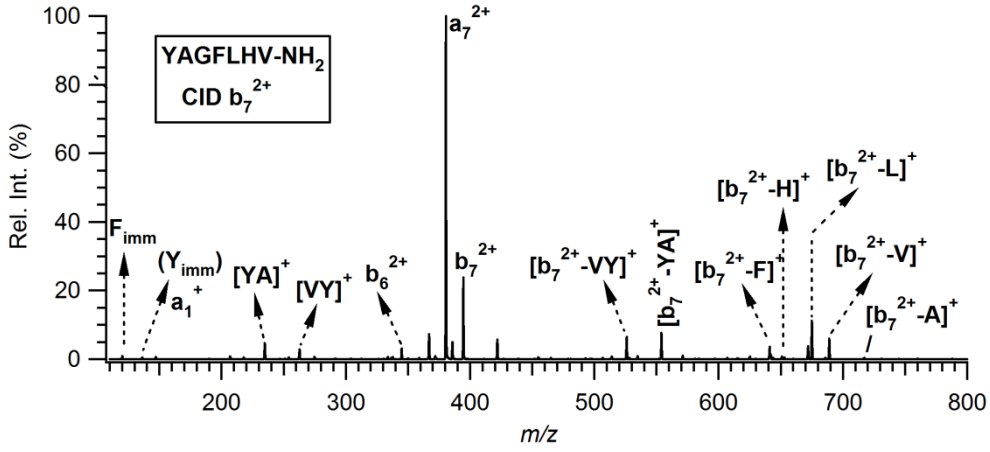

Figure 4.6. CID mass spectra of YAGFLHV-NH_2

When examining CID of YAGFLHV-NH_2 spectrum doubly-protonated amino acids a_7^{2+} (*m*/z 380.5) and b_6^{2+} (*m*/*z* 345) signals were seemed, illustrated in Figure 4.6. On the other hand, still internal amino acid eliminations were observed, namely $[b_7^{2+}\text{-A}]^+$ (*m*/*z* 717.0), $[b_7^{2+}\text{-V}]^+$ (*m*/*z* 689.0), $[b_7^{2+}\text{-L}]^+$ (*m*/*z* 675.0), $[b_7^{2+}\text{-H}]^+$ (*m*/*z* 651.0),

$[b_7^{2+}\text{-F}]^+$ (*m*/*z* 641.0), $[b_7^{2+}\text{-YA}]^+$ (*m*/*z* 554.0), $[b_7^{2+}\text{-VY}]^+$ (*m*/*z* 526.0), $[\text{VY}]^+$ (*m*/*z* 263.0), $[\text{YA}]^+$ (*m*/*z* 235.0), Y_{imm} (*m*/*z* 136.0), and F_{imm} (*m*/*z* 120.0).

His residue was positioned at the C-terminal and it was continuing to seem singly-protonated internal amino acid eliminations such as $[b_7^{2+}\text{-V}]^+$ (*m*/*z* 689.0), $[b_7^{2+}\text{-L}]^+$ (*m*/*z* 675.0), $[b_7^{2+}\text{-H}]^+$ (*m*/*z* 651.0), $[b_7^{2+}\text{-F}]^+$ (*m*/*z* 641.0), $[b_7^{2+}\text{-Y}]^+$ (*m*/*z* 625.0), $[b_7^{2+}\text{-VL}]^+$ (*m*/*z* 576.0), $[b_7^{2+}\text{-YA}]^+$ (*m*/*z* 554.0), $[\text{YA}]^+$ (*m*/*z* 235.0), $[\text{VL}]^+$ (*m*/*z* 213.0), Y_{imm} (*m*/*z* 136.0), and F_{imm} (*m*/*z* 120.0). On the other hand, direct sequence fragments namely b_7^*(*m*/*z* 386.0) and a_7^{2+} (m/*z* 380.5) were observed at the spectrum (see Figure 4.7).

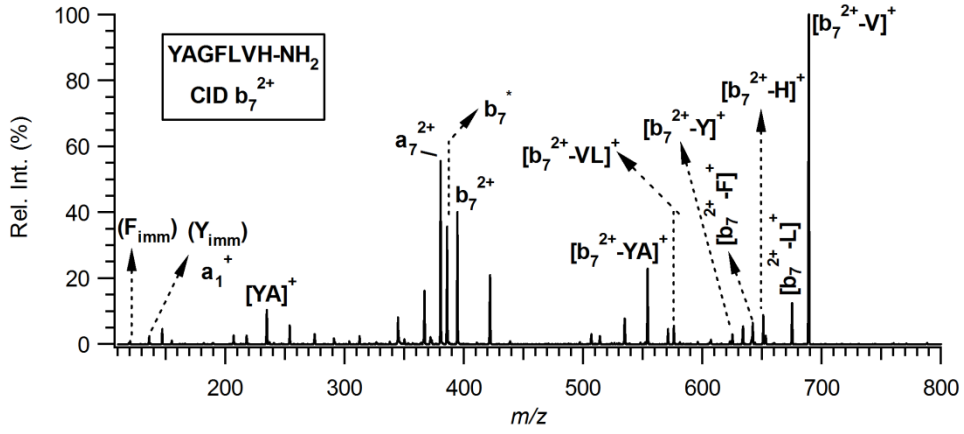

Figure 4.7. CID mass spectra of YAGFLVH-NH_2

Based upon to the whole mass spectra of YAGFLV-NH_2 series which containing His residue at the all positions from N-terminal to the C-terminal a new mechanism was proposed. The fragmentation reaction mechanism of $[M+2H]^{2+}$ ion of YAGFHLV-NH_2 are shown in Figure 4.8. YAGFHLV-NH_2 peptide was chosen as an example for explaining the mechanism.

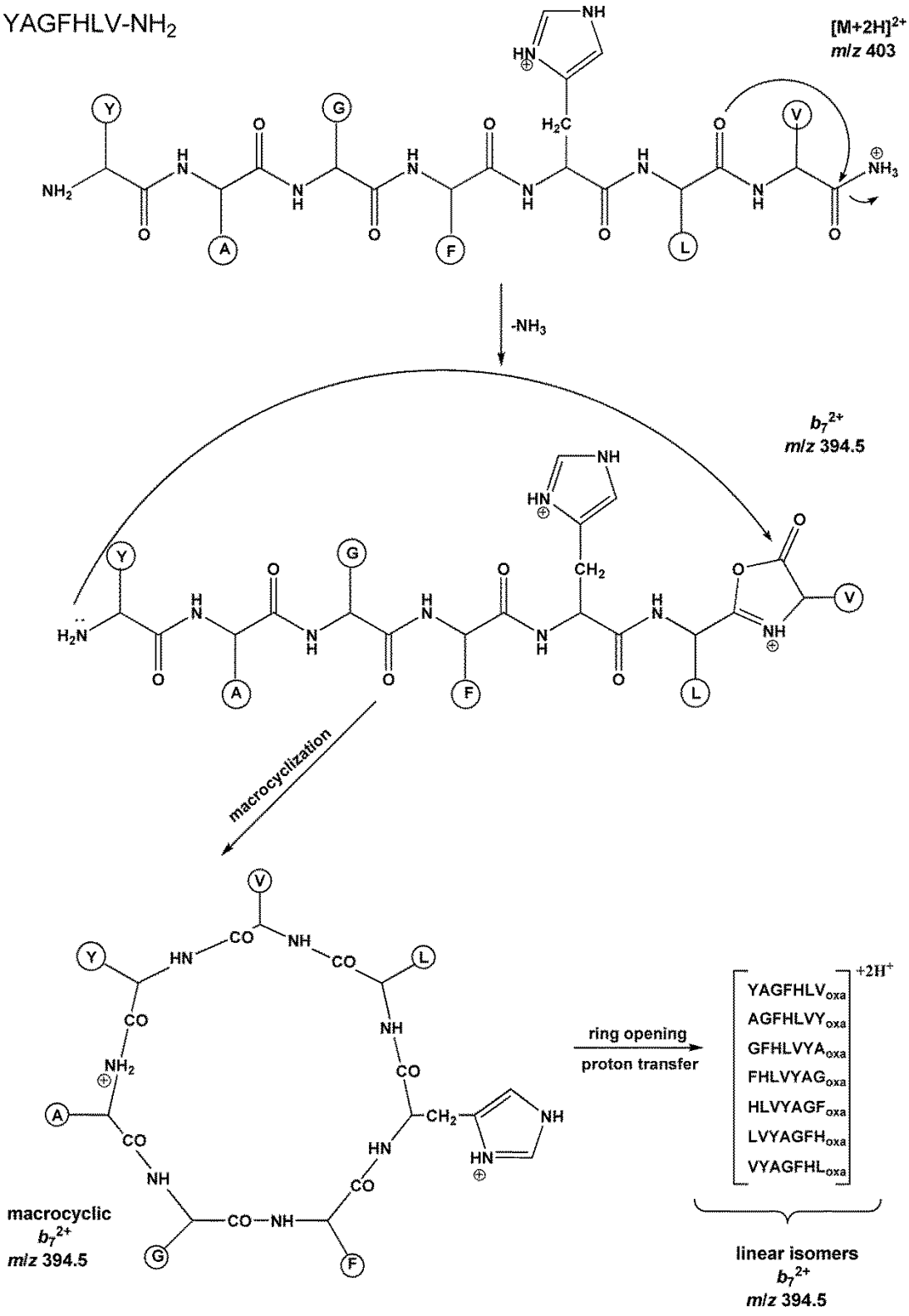

Figure 4.8. Proposed reaction mechanism for the formation of macrocyclic b_7^{2+} ion in the gas-phase

The first structure indicates doubly-protonated form of YAGFHLV-NH_2 at *m*/*z* 403.0 where *z* equals to two. The first proton is positioned to the side chain of His residue while the second proton is located at the C-terminal amine group.

Afterwards, the ammonia is lost (-17 Da) from $[M+2H]^{2+}$ ion via nucleophilic attack of carbonyl oxygen to the next carbonyl carbon which then leads to the formation of protonated five membered oxazolone ring at the C-terminal end of the peptide. The generated doubly-protonated b_7^{2+} ion undergoes macrocyclization reaction in the gas-phase. The macrocyclic structure may undergo numerous ring-opening pathways to form seven different b_7^{2+} isomers; all possess a C-terminal oxazolone group.

As an illustration, b_7^{2+} $YAGFHLV_{oxa}$ isomer is selected for representation of its gas-phase fragmentation chemistry (Figure 4.9).

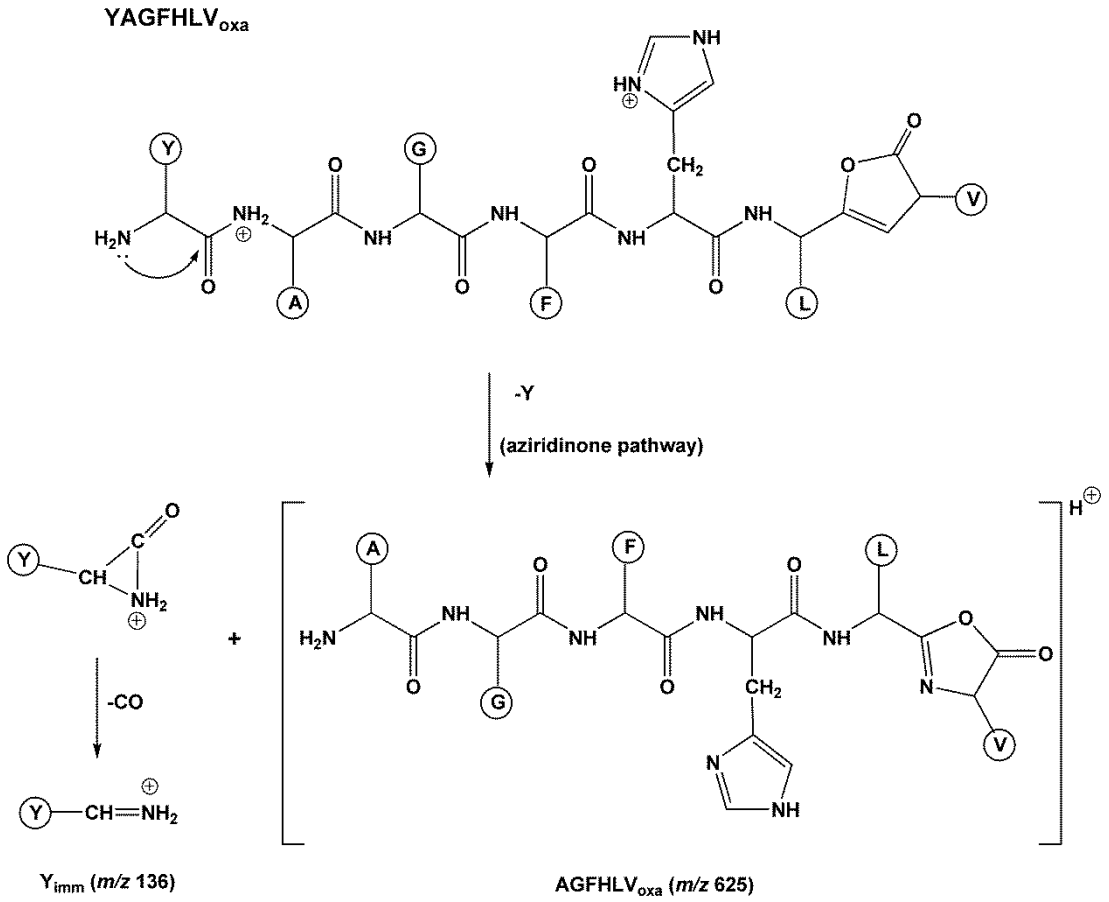

Figure 4.9. Formation of protonated N-terminal iminium ion and singly-protonated internal b_6^+ ion

The N-terminal amino acid of the peptide is cleaved via aziridinone pathway. Meantime, the protonated AGFHLV$_{oxa}$ is formed. The formed aziridinone fragment can further loose CO (-28) to generate Y$_{imm}$ (*m*/*z* 136.0) ion (see Figure 4.5).

4.2.2. His Residue Containing AAAAAA-NH$_2$ Peptide Series

In this section, CID of b_7^{2+} (*m*/*z* 282.5) of HAAAAAA-NH$_2$, AHAAAAA-NH$_2$, AAHAAAA-NH$_2$, AAAHAAA-NH$_2$, AAAAHAA-NH$_2$ and also MS^3 analysis of water-loss fragment ion (*m*/*z* 282.0) of AAAAAHA-NH$_2$ and AAAAAAH-NH$_2$ heptapeptides were performed. This series were chosen to compare similarities and differences of behavior of His residue between C-terminal amidated YAGFLV and AAAAAA series.

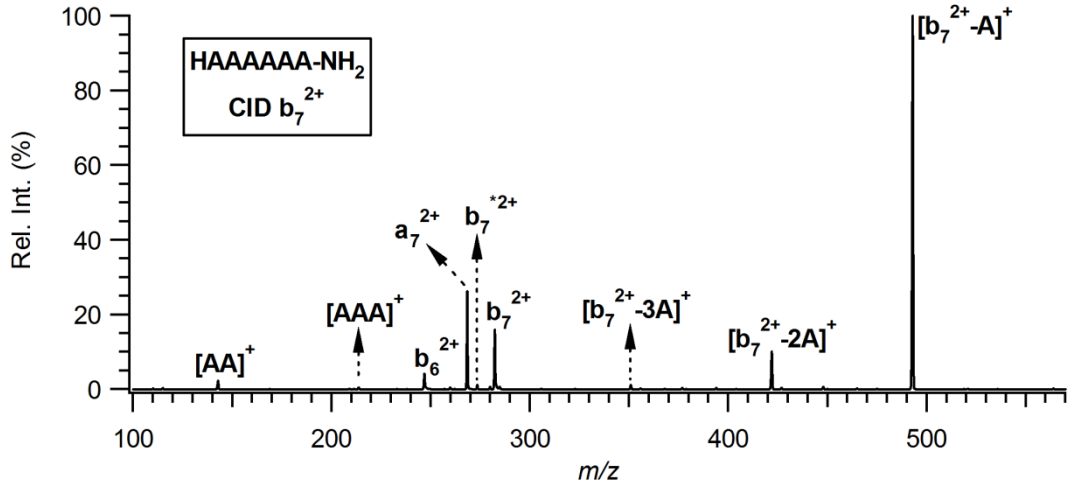

Figure 4.10. CID mass spectrum of b_7^{2+} ion of HAAAAAA-NH$_2$

In Figure 4.10, doubly-protonated b_7 ion CID mass spectrum of HAAAAAA-NH$_2$ was examined. The peak at *m*/*z* 493.0 was observed as Ala elimination from b_7^{2+} (*m*/*z* 282.5). In the meantime, $[b_7^{2+}\text{-}2A]^+$ (*m*/*z* 422.0), $[b_7^{2+}\text{-}3A]^+$ (*m*/*z* 351.0), and $[AAA]^+$ (*m*/*z* 215.0), $[AA]^+$ (*m*/*z* 143.0) fragmentations were obtained under low energy CID conditions. But then, the ions; $[b_7^{2+}\text{-}A]^+$ (*m*/*z* 493.0), $[b_7^{2+}\text{-}2A]^+$ (*m*/*z* 422.0), and $[b_7^{2+}\text{-}3A]^+$ (*m*/*z* 351.0) coincide with b_6^+, b_5^+, and b_4^+ direct sequence ions, respectively. Besides, direct sequence ions a_7^{2+} (*m*/*z* 268.5) and b_6^{2+} (*m*/*z* 247.0) were obtained which compatible with HYAGFLV-NH$_2$ model peptide.

Figure 4.11 shows that the fragmentation patterns of the *m/z* 282.5 ions derived from C-terminal amidated Ala containing heptapeptides (AHAAAAA-NH_2, AAHAAAA-NH_2, AAAHAAA-NH_2, and AAAAHAA-NH_2) demonstrates entirely the same product ions in their CID mass spectra.

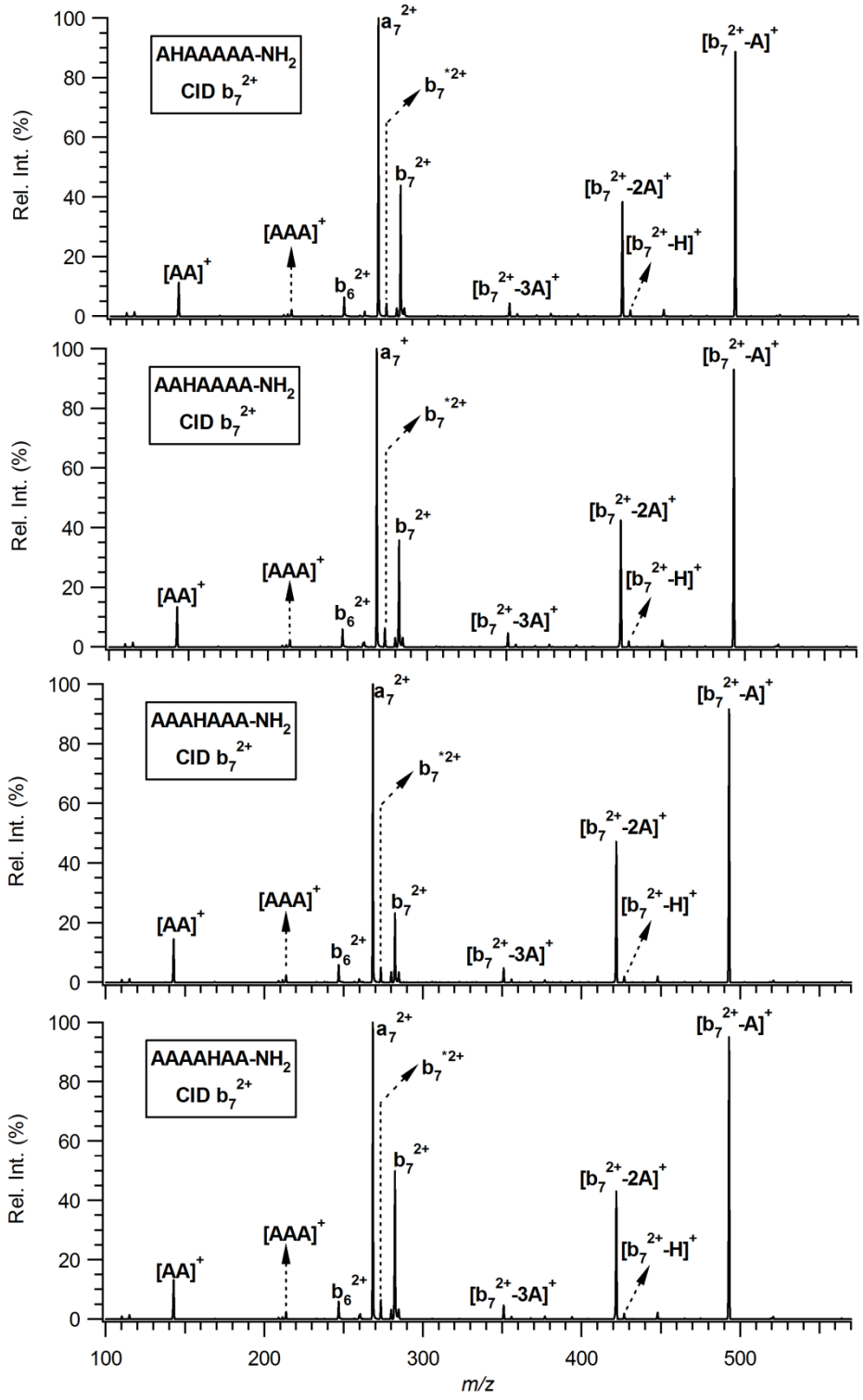

Figure 4.11. Comparison of b_7^{2+} ion CID mass spectra of AHAAAAA-NH_2, AAHAAAA-NH_2, AAAHAAA-NH_2 and AAAAHAA-NH_2

The fragment ions $[b_7^{2+}\text{-A}]^+$ (*m*/*z* 493.0), $[b_7^{2+}\text{-2A}]^+$ (*m*/*z* 422.0), and $[b_7^{2+}\text{-3A}]^+$ (*m*/*z* 351.0) exhibited same distribution in all four spectra and these ions equal to b_6^+, b_5^+, b_4^+ direct sequence ions, respectively for mentioned peptides except AAAAHAA-NH_2 which b_4^+ ion represents at *m*/*z* 285.0 peak. And also, the most intense fragment ion is a_7^{2+} (*m*/*z* 268.5) which is in competition with $[b_7^{2+}\text{-A}]^+$ (*m*/*z* 493.0) ion. The peak at *m*/*z* 214.0 indicates $[AAA]^+$ and *m*/*z* 143.0 indicates $[AA]^+$ internal elimination which are one each evidence for macrocyclization. Moreover His elimination named $[b_7^{2+}\text{-H}]^+$ (*m*/*z* 427.0) was observed more distinct which is another evidence for macrocyclization.

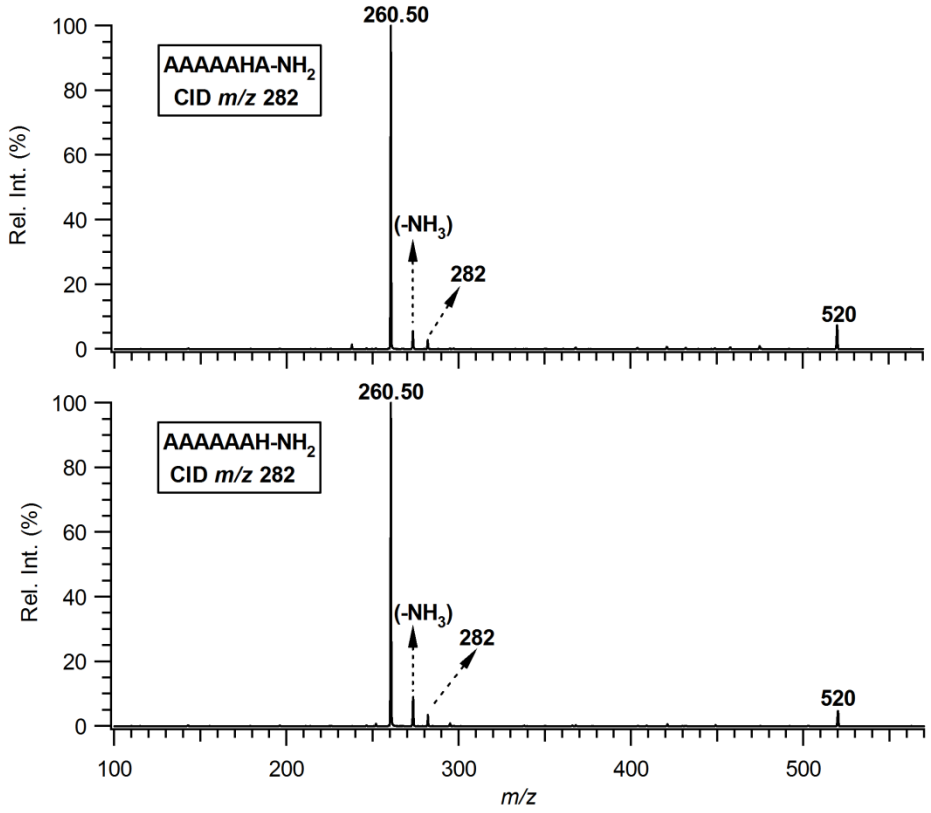

Figure 4.12. Comparison of *m*/*z* 282.0 $[[M+2H]\text{-}H_2O]^{2+}$ ion CID mass spectra of AAAAAHA-NH_2 and AAAAAAH-NH_2

Thus far MS/MS ($[M+2H)^{2+}$) CID mass spectra of whole heptapeptides formed b_7^{2+} (*m*/*z* 282.5) but MS/MS CID of last two peptides generated an ion at *m*/*z* 282.0 instead of *m*/*z* 282.5. Moreover fragment ions of this ion very different from b_7^{2+} ion's (Figure 4.12). This situation show that His residue fixes a proton on its side chain and another proton takes place C-terminal amidated nitrogen and these two same type charges close to each other, C-N cleavage becomes harder and b_7^{2+} ion cannot be

generated. However, this Coulombic repulsion was not observed in YAGFLV series. On the other hand, it is possible that explaining this water-loss process, instead of NH_3 elimination, with specific behavior of Ala and His residues.

4.3. Investigation of Macrocyclic Behavior of Doubly-Protonated b_8 Ions

In previous sections, CID mass spectra of C-terminal amidated heptapeptides were examined and based upon the behavior of doubly-protonated b_7 ion a new mechanism was proposed. In this section, some peptides were chosen from the literature[39], namely, SHIGDAVVI-OH, EHAGVISVL-OH, SVEHAGVIL-OH, and GRIDKPILK-OH for research into behavior of doubly-protonated b_8 ion. The results were compared with previous results.

4.3.1. SHIGDAVVI-OH

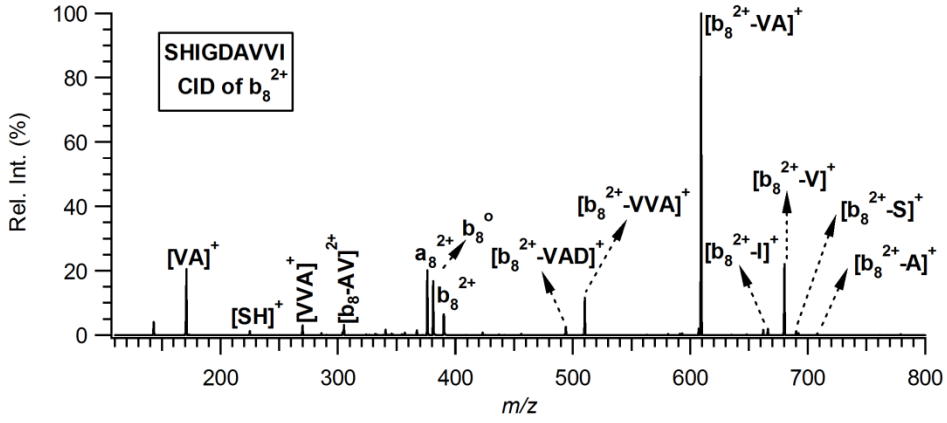

Figure 4.13. CID mass spectrum of b_8^{2+} ion of SHIGDAVVI-OH

In this part, CID MS spectrum of b_8^{2+} ion (*m*/*z* 390.0) derived from SHIGDAVVI-OH peptide was examined. Direct sequence ions that water-loss from b_8^{2+} ion was symbolised as b_8^{o} (*m*/*z* 381.0) and a_8^{2+} (*m*/*z* 376.0) ions which was CO loss from b_8^{2+} ion were obtained, prominently. Moreover, singly-protonated internal amino acid(s) eliminations were obtained such as $[b_8^{2+}\text{-A}]^+$ (*m*/*z* 708.0), $[b_8^{2+}\text{-S}]^+$ (*m*/*z* 692.0), $[b_8^{2+}\text{-V}]^+$ (*m*/*z* 680.0), $[b_8^{2+}\text{-I}]^+$ (*m*/*z* 666.0), $[b_8^{2+}\text{-VA}]^+$ (*m*/*z* 609.0), $[b_8^{2+}\text{-VVA}]^+$ (*m*/*z*

510.0), $[b_8^{2+}\text{-VAD}]^+$ (*m*/*z* 494.0). Meantime, singly-potonated double and triple amino acids were observed as follows $[\text{VVA}]^+$ (*m*/*z* 270.0), $[\text{SH}]^+$ (*m*/*z* 225.0), and $[\text{VA}]^+$ (*m*/*z* 171.0).

4.3.2. EHAGVISVL-OH & SVEHAGVIL-OH

EHAGVISVL-OH and SVEHAGVIL-OH are isomer peptides and their CID MS spectra of doubly-protonated b_8 (*m*/*z* 397.0) ion fragmentation showed the same ion distribution, illustrated in Figure 4.14.

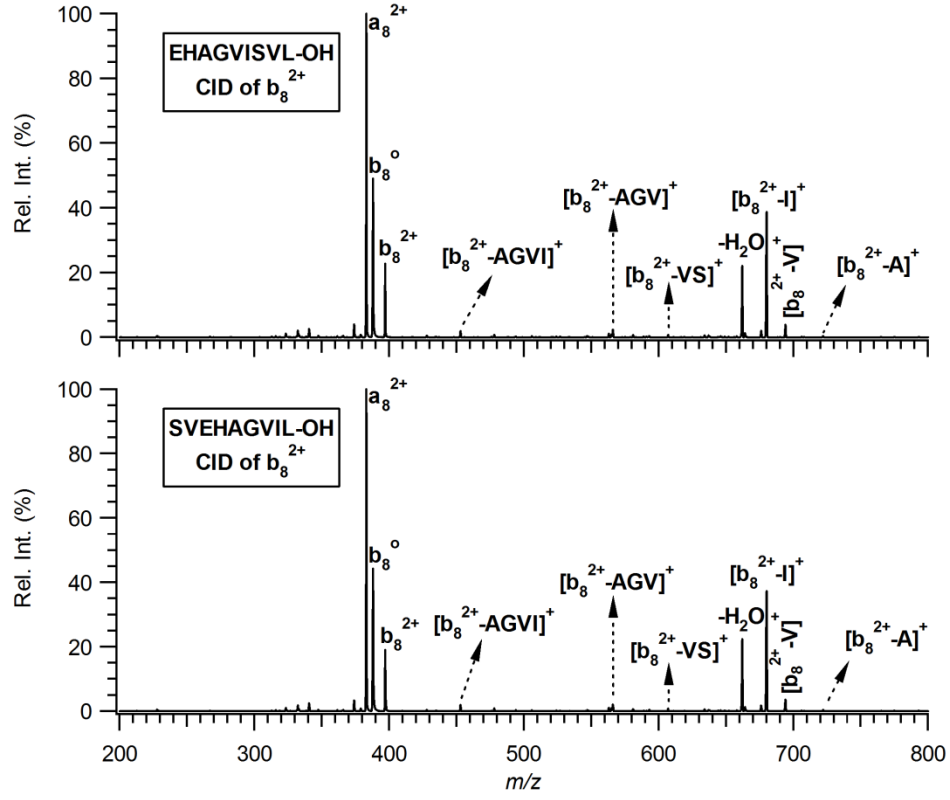

Figure 4.14. Comparison of CID mass spectra of b_8^{2+} ion of EHAGVISVL-OH and SVEHAGVIL-OH

Direct sequence ions at the peak *m*/*z* 388.0 (water-loss from b_8^{2+}) and *m*/*z* 383.0 (CO elimination from b_8^{2+}) were recorded. In addition, single amino acid eliminations namely $[b_8^{2+}\text{-A}]^+$ (*m*/*z* 722.0), $[b_8^{2+}\text{-V}]^+$ (*m*/*z* 694.0), $[b_8^{2+}\text{-I}]^+$ (*m*/*z* 680.0), and also multiple amino acid eliminations, namely $[b_8^{2+}\text{-VS}]^+$ (*m*/*z* 607.0) $[b_8^{2+}\text{-AGV}]^+$ (*m*/*z* 566.0), and $[b_8^{2+}\text{-AGVI}]^+$ (*m*/*z* 453.0) were obtained.

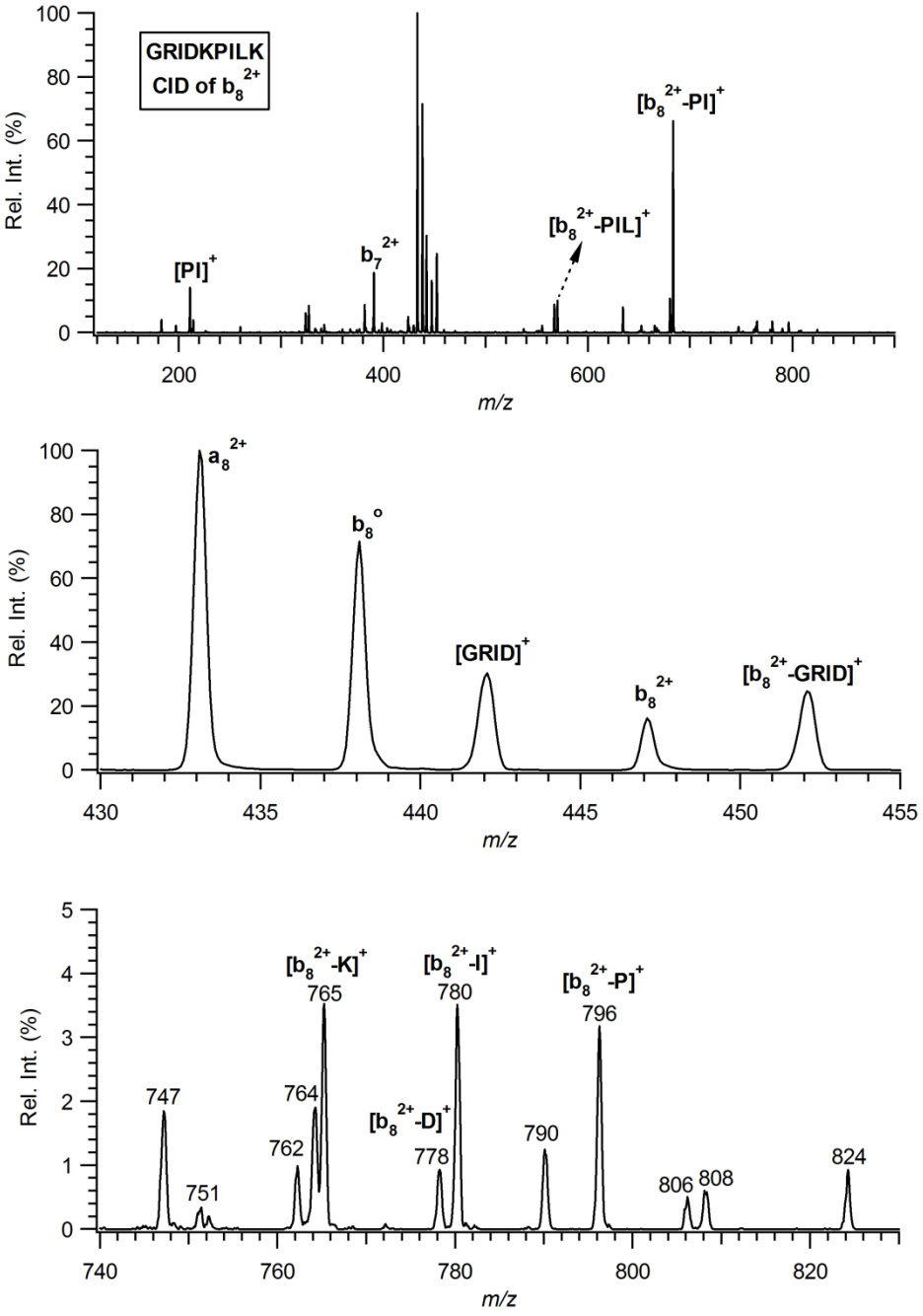

Figure 4.15. CID mass spectra b_8^{2+} ion of GRIDKPILK-OH

The fragment at *m*/*z* 680.0 refers to b_7^+ which is a direct sequence ion for SVEHAGVIL but does not for EHAGVISVL. However this peak was obtained both peptides with a significant intensity. This results provide solid evidence for the macrocyclization.

4.3.3. GRIDKPILK-OH

The last peptide which was used for examining behavior of fragmentation of b_8^{2+} ion is C-terminal free acid GRIDKPILK. Its mass spectrum is illustrated in Figure 4.15. Above-mentioned peptide includes more than one basic amino acids; Arg (R) and Lys (K) residues. However, their positions do not much closer to each other. Therefore, it is thought that its CID mass spectrum is more complicated than the others. On the other hand, non-sequence ions were obtained such as $[b_8^{2+}\text{-P}]^+$ (*m*/*z* 796.0), $[b_8^{2+}\text{-I}]^+$ (*m*/*z* 780.0), $[b_8^{2+}\text{-D}]^+$ (*m*/*z* 778.0), $[b_8^{2+}\text{-K}]^+$ (*m*/*z* 765.0), $[b_8^{2+}\text{-PI}]^+$ (*m*/*z* 683.0), $[b_8^{2+}\text{-PIL}]^+$ (*m*/*z* 570.0), and $[b_8^{2+}\text{-GRID}]^+$ (*m*/*z* 452.0). Complementary fragment of $[b_8^{2+}\text{-GRID}]^+$ (*m*/*z* 452.0) and $[b_8^{2+}\text{-PI}]^+$ (*m*/*z* 683.0) also were observed which were $[\text{GRID}]^+$ (*m*/*z* 442.0) and $[\text{PI}]^+$ (*m*/*z* 211.0), respectively.

4.4. Investigation of Macrocyclic Behavior of Doubly-Protonated b_9 Ion

KRNGVIIAGY-OH decapeptides was used for examining behavior of doubly charged b_9 ion. The mentioned peptide was found from literature[39] such as other C-terminal free acid nonapeptides.

4.4.1. KRNGVIIAGY-OH

CID of MS^3 spectrum of KRNGVIIAY-OH peptide had a good deal of internal amino acid eliminations such as $[b_9^{2+}\text{-A}]^+$ (*m*/*z* 838.0), $[b_9^{2+}\text{-V}]^+$ (*m*/*z* 810.0), $[b_9^{2+}\text{-I}]^+$ (*m*/*z* 796.0), $[b_9^{2+}\text{-IA}]^+$ (*m*/*z* 725.0), and $[b_9^{2+}\text{-II}]^+$ (*m*/*z* 683.0), illustrated in Figure 4.16.

Surprisingly, doubly-protonated fragment ions were recorded such as $[b_9\text{-A}]^{2+}$ (*m*/*z* 419.5), $[b_9\text{-V}]^{2+}$ (*m*/*z* 405.5), $[b_9\text{-I}]^{2+}$ (*m*/*z* 398.5), $[b_9\text{-K}]^{2+}$ (*m*/*z* 391.0), $[b_9\text{-AI}]^{2+}$ (*m*/*z* 363.0), and $[b_9\text{-II}]^{2+}$ (*m*/*z* 342.0). It is possible that these signals were obtained because two basic amino acid residues (Lys and Arg) were abreast positioned. From this point of view proposed mechanism was adjusted and a new mechanism was suggested (Figure 4.17).

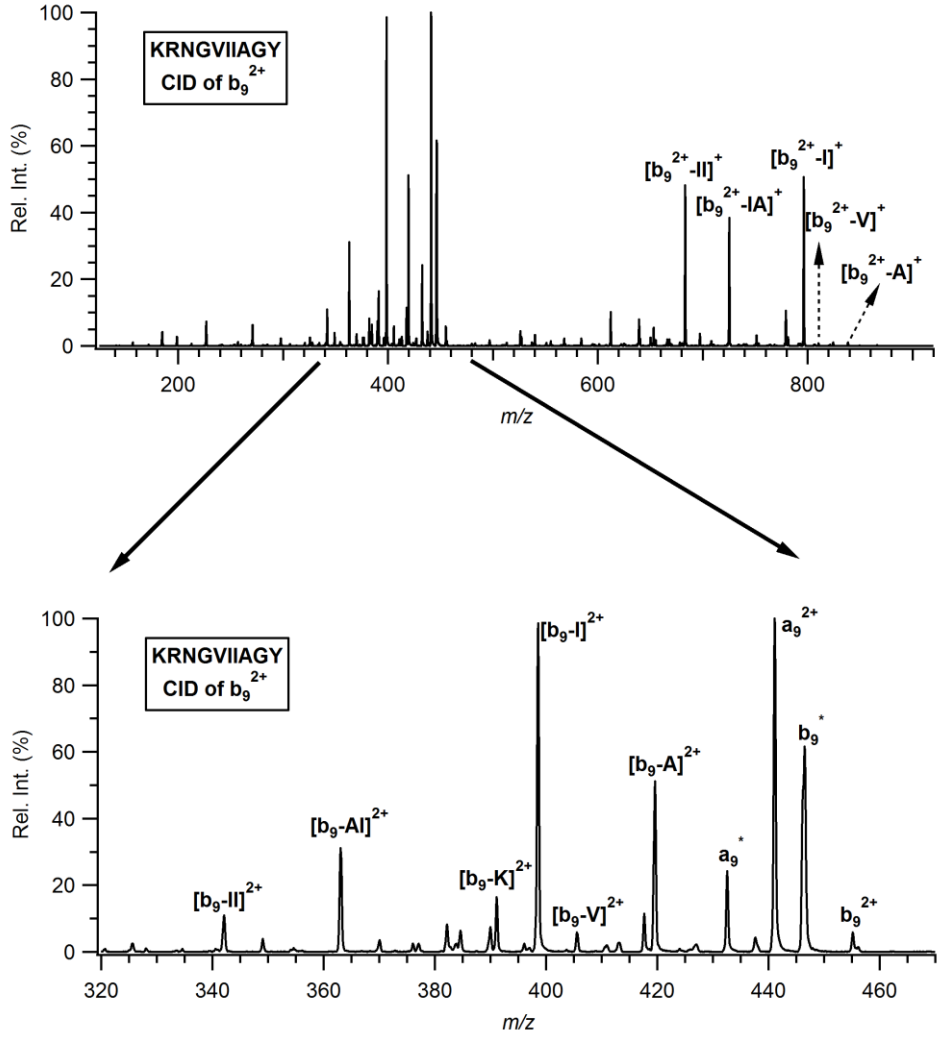

Figure 4.16. CID mass spectrum of b_9^{2+} ion KRNGVIIAGY-OH

The ten amino acid containing peptide loses water (-H_2O) and Tyr (-Y) residue immediately and linear oxazolone b_9^{2+} ion is formed. After the head-to-tail cyclization macrocyclic b_9^{2+} ions was come into existence. In consequence of ring opening process nine, doubly-protonated, linear oxazolone isomers were obtained. To explain the rest of the mechanism $GKRNGVIIA_{oxa}$ isomer was choosen. One of the charge is fixed on the Arg side chain, because of its higher basicity, and other one is on the C-terminal oxazolone form of Ala. Subsequently, Ala residue is loosed and $GKRNGVII_{oxa}$ structure is formed which has two protons on its on. It is possible that one of the charge is fixed on Arg residue and other is mobile.

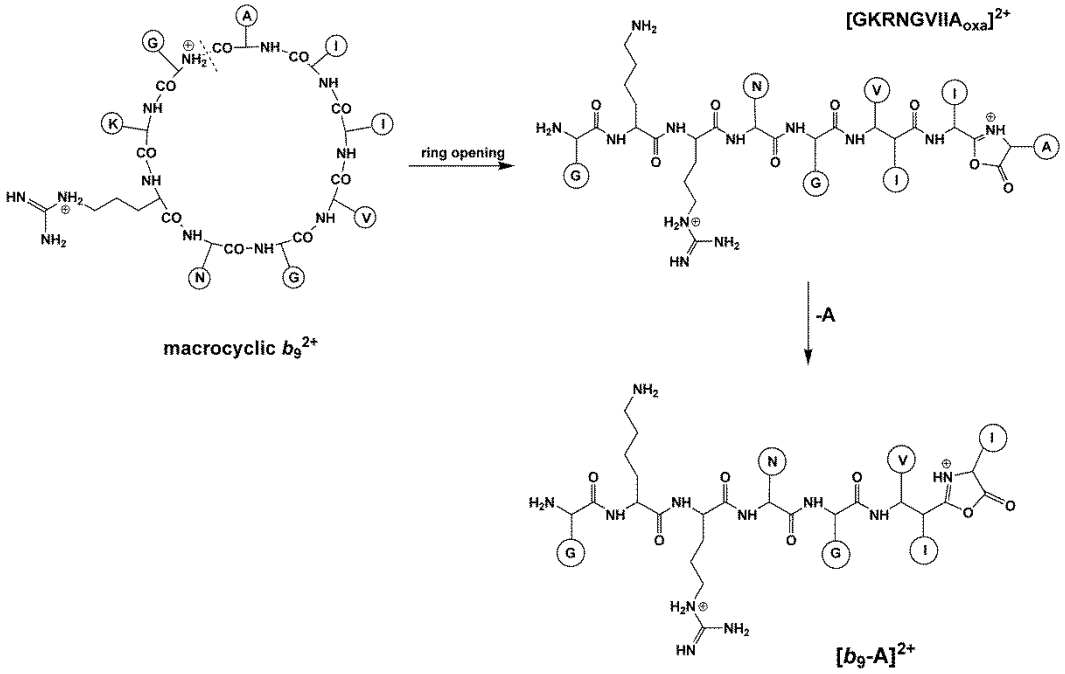

Figure 4.17. Proposed reaction mechanism for the formation of $[b_9\text{-A}]^{2+}$ ion in the gas-phase

4.5. Results and Discussions

Three different doubly-protonated *b* ions were examined using different model peptide series with variety of amino acid sequencing. The general aspect of the CID spectra of doubly-protonated *b* ions gave the similar behavior. Based upon the results two mechanisms were proposed relevant the macrocyclic behavior of doubly-protonated *b* ions. Interesting results were observed just only in AAAAAHA-NH_2, AAAAAAH-NH_2, and KRNGVIIAGY-OH model peptides.

Firstly, YAGFLV-NH_2 model peptide series was used because of their most common usage in our studies. His residue was put to use for creating doubly-protonated peptides. To investigate position and amino acid effect of His residue was located from N-terminal to C-terminal, namely HYAGFLV-NH_2, YHAGFLV-NH_2, YAHGFLV-NH_2, YAGHFLV-NH_2, YAGFHLV-NH_2, YAGFLHV-NH_2, and YAGFLVH-NH_2. The CID mass spectra of b_7^{2+} ions derived from His containing YAGFLV-NH_2 series exhibited the similar internal amino acid eliminations which can be accepted an evidence for macrocyclization of *b* ions. Based upon the this behaviour a new reaction mechanism account for the formation of internal amino acid losses. According to the mechanism under low CID conditions doubly-protonated peptide ($[M+2H]^{2+}$ *m*/*z* 403.0)

loses NH_3 group and a doubly-protonated linear oxazolone b_7^{2+} ion is formed. In the sequel, amine nitrogen attacks to the carbonyl carbon of the C-terminal oxazolone group and "head-to-tail" cyclization comes true. After the ring opening process (according to the mobile proton position) linear oxazolone isomers are generated. Subsequently, amine nitrogen attacks to the next amino acid carbonyl carbon. Ultimately, by following aziridinone pathway an iminium ion and an internal singly-protonated *b* ion are formed.

Secondly, AAAAAA-NH_2 model peptides series were used which including His residue from N-termini to C-termini, namely HAAAAAA-NH_2, AHAAAAA-NH_2, AAHAAAA-NH_2, AAAHAAA-NH_2, AAAAHAA-NH_2, AAAAAHA-NH_2, and AAAAAAH-NH_2. Ala is one of the less reactive amino acid and this is the reason why the mentioned model pentapeptide series was used. The mass spectra of these series were examined under low CID conditions. In general, three different spectra were obtained. The first one belongs to HAAAAAA-NH_2 peptide where internal singly-protonated single-Ala, double-Ala, and triple-Ala eliminations were observed. The second different spectra belong to C-terminal amidated AHAAAAA, AAHAAAA, AAAHAAA, and AAAAHAA series. The four spectra showed the nearly the same fragment signals which were singly-protonated single-Ala, double-Ala, triple-Ala, and His eliminitaions come from CID of b_7^{2+} ion. This is an evidence for macrocyclizaition reaction. Due to the same internal amino acid eliminations were obtained from YAGFLV-NH_2 series the proposed mechanism is valid for His residue containing AAAAAA-NH_2 series, too. On the other hand, the same spectra were not obtained in MS^3 CID of C-terminal amidated YHAGFLV, YAHGFLV, YAGHFLV, and YAGFHLV model peptides. This results were shown that basic amino acid behaviour is affected from neighbour amino acid residues. The third different spectra belong to AAAAAHA-NH_2 and AAAAAAH-NH_2 pentapeptide series. The MS/MS spectra of these peptides could not form NH_3 elimination and water-loss fragment (*m*/*z* 282.0) was observed instead of b_7^{2+} ion formation. So, the CID mass spectra of the ion (*m*/*z* 282.0) showed very different fragment ions than the others. This results are evidences of a charge is fixed on the His side chain. Depending upon the Coulombic repulsion linear oxazolone could not be formed and the reaction mechanism follows another pathway.

In another section, different sequenced model peptides were used namely, SHIGDAVVI-OH, EHAGVISVL-OH, SVEHAGVIL-OH, and GRIDKPILK-OH, which were matched with a cell line sequences, to examining behaviour of doubly-protonated b_8 ion. Several internal amino acids eliminations were monitored in CID

mass spectra of doubly-charged b_8 ions for all peptides. These eliminations support the proposed mechanism because observing non-direct sequence ions were not observed derived from singly-charged *b* ions of mentioned peptides. Especially, it was a proof that generating same fragment ions from CID of MS^3 EHAGVISVL-OH and SVEHAGVIL-OH peptides since they are isomers and their macrocyclic forms are entirely the same.

To compare macrocyclic behaviour of more larger doubly-protonated *b* ion KRNGVIIAGY-OH peptide was examined which is matched again fragment of the same cell line. An surprising behaviour was observed via tandem MS. Doubly-protonated internal amino acid eliminitaions were obtained meanwhile singly-protonated internal amino acid eliminations. From this point of view, the mechanism was adjusted and a new pathway was suggested. The process is the same with the first proposed mechanism until the linear doubly-protonated oxazolone structure formation which is formed after reopening pathway. After that, internal elimination was observed from the C-terminal oxazolone structure and doubly-protonated internal amino acid elimination was generated. Most probably it was come true because two basic amino acids very closer to each other and and the pathways follow C-terminal elimination pathway instead of aziridinone pathway. In consequence, doubly-protonated ion is formed that one of the charged is fixed on the most basic amino acid Arg side chain and the other is mobile.

CHAPTER 5

CONCLUSION

In this studies, two sets of C-terminal amidated model peptides that HYAGFLV-NH_2, YHAGFLV-NH_2, YAHGFLV-NH_2, YAGHFLV-NH_2, YAGFHLV-NH_2, YAGFLHV-NH_2, YAGFLVH-NH_2 and HAAAAAA-NH_2, AHAAAAA-NH_2, AAHAAAA-NH_2, AAAHAAA-NH_2, AAAAHAA-NH_2, AAAAAHA-NH_2, AAAAAAH-NH_2 where the position of the histidine (His) residue is varied from N-to-C-terminal were used to investigate the macrocyclic behaviour of doubly protonated b_n (n=7, 8, and 9) ions. It was observed that doubly-protonated b_7 ions produced from these peptides forms a head-to-tail macrocyclization of the corresponding b_7 ions except the peptides sequences: AAAAAHA-NH_2 and AAAAAAH-NH_2. Instead of NH_3 elimination to form b_7 ions from parent ions, H_2O elimination was observed from these two peptides. As it is known the formation of linear oxazolone is always followed by head-to-tail cyclization to end up macrocyclic larger *b* ions. It was shown that b_2 ions produced from HA or AH showed diketopiperazine, not the oxazolone. This could be the reason of not to observed macrocyclic *b* ions when the b_7 ions produced from AAAAAHA-NH_2 and AAAAAAH-NH_2 peptides. It might be produced linear diketopiperazine instead of linear oxazolone b_7 ions and that could be the reason to show H_2O elimination instead of NH_3 elimination from parent ions. As a result, completely different MS/MS spectra was observed for these two peptides. This result showed that b_7 ions produced from AAAAAHA-NH_2 and AAAAAAH-NH_2 have different structures then the b_7 ions produced from HAAAAAA-NH_2, AHAAAAA-NH_2, AAHAAAA-NH_2, AAAHAAA-NH_2, AAAAHAA-NH_2.

In addition that b_8 and b_9 ions were used to examine the behaviour of larger doubly-protonated *b* ions. The MS/MS spectra of b_8 ions produced from SVEHAGVIL-OH, SHIGDAVVI-OH, EHAGVISVL-OH, and GRIDKPILK-OH showed internal amino acid elimination and it is known that this is the evidence of macrocyclization behavior of *b*-type ions. A new fragmentation mechanism was proposed for internal amino acid elimination for doubly-protonated *b*-type ions. It was proposed that, after forming macrocyclic doubly-protonated *b*-ions, that the ring was reopened and several

linear oxazolone isomers were formed under the low CID condition, N-terminal amino acids were eliminated as protonated iminium ion and also singly-protonated b_6^+ ion were formed.

The MS/MS spectra of b_9 ions produced from KRNGVIIAGY-OH also show internal amino acid elimination which is evidence of macrocyclization. However, the fragmentation behavior of b_9^{2+} ions was different than the b_7^{2+} and b_8^{2+} ions. The doubly-protonated b_8 ions were observed after elimination of internal amino acid from b_9 ions. This could be the reason of multiple basic amino acids which are attached to each other. The protons might be staying most of the time on these basic amino acid residues.

REFERENCES

1. Thomson, J. J., Cathode Rays. *Philos Mag* **1897,** *44*, 293-316.

2. Bleakney, W., A New Method of Positive Ray Analysis and Its Application to the Measurement of Ionization Potentials in Mercury Vapor. *Physical Review* **1929,** *34* (1), 157-160.

3. Munson, M. S. B.; Field, F. H., Chemical Ionization Mass Spectrometry. II. Esters. *Journal of the American Chemical Society* **1966,** *88* (19), 4337-4345.

4. Beckey, H. D., Principles of Field Ionization and Field Desorption Mass Spectrometry. 1977.

5. Macfarlane, R. D.; Torgerson, D. F., *Science* **1976,** *191*, 920-925.

6. Barber, M.; Bordoli, R. S.; Sedgwick, R. D.; Tyler, A. N., Fast atom bombardment of solids as an ion source in mass spectrometry. *Nature* **1981,** *293* (5830), 270-275.

7. (a) Dole, M. M., L. L.; Hines, R. L., Molecular beams of macroions. *J Chem Phys* **1968,** *49* (5), 2240-2249; (b) Whitehouse, C. M.; Dreyer, R. N.; Yamashita, M.; Fenn, J. B., Electrospray Interface for Liquid Chromatographs and Mass Spectrometers. *Anal Chem* **1985,** *57* (3), 675-679; (c) Yamashita, M.; Fenn, J. B., Electrospray Ion-Source - Another Variation on the Free-Jet Theme. *J Phys Chem-Us* **1984,** *88* (20), 4451-4459.

8. (a) Karas, M.; Hillenkamp, F., Laser Desorption Ionization of Proteins with Molecular Masses Exceeding 10000 Daltons. *Anal Chem* **1988,** *60* (20), 2299-2301; (b) Tanaka, K.; Waki, H.; Ido, Y.; Akita, S.; Yoshida, Y.; Yoshida, T.; Matsuo, T., Protein and polymer analyses up to m/z 100 000 by laser ionization time-of-flight mass spectrometry. *Rapid Communications in Mass Spectrometry* **1988,** *2* (8), 151-153.

9. Fenn, J. B.; Mann, M.; Meng, C. K.; Wong, S. F.; Whitehouse, C. M., Electrospray Ionization for Mass-Spectrometry of Large Biomolecules. *Science* **1989,** *246* (4926), 64-71.

10. Liebler C. Introduction to Proteomics Tools for the New Biology, Humana Press: Totowa, **2002**.

11. Taylor, G. I., Disintegration of Water Droplets in an Electric Field. *Proc. R. Soc.* **1964,** *A* (8), 678-686.

12. Paul, W. S., H., Ein neues Massenspektrometer ohne Magnetfeld. *Z. Naturforschg* **1953,** *8A*, 448-450.

13. Stafford Jr, G. C.; Kelley, P. E.; Syka, J. E. P.; Reynolds, W. E.; Todd, J. F. J., Recent improvements in and analytical applications of advanced ion trap technology. *Int J Mass Spectrom* **1984,** *60* (1), 85-98.

14. Douglas, D. J.; Frank, A. J.; Mao, D., Linear ion traps in mass spectrometry. *Mass Spectrom Rev* **2005,** *24* (1), 1-29.

15. Louris, J. N.; Brodbelt-Lustig, J. S.; Graham Cooks, R.; Glish, G. L.; van Berkel, G. J.; McLuckey, S. A., Ion isolation and sequential stages of mass spectrometry in a quadrupole ion trap mass spectrometer. *Int J Mass Spectrom* **1990,** *96* (2), 117-137.

16. Stephens, W. E., A Pulsed Mass Spectrometer with Time Dispersion. *Phys Rev A* **1946,** *69*, 691.

17. Wiley, W. C. M., J. B., Time-of-Flight Mass Spectrometer with Improved Resolution. *Rev. Sci. Instrum.* **1955,** *16*, 1150-1157.

18. Dass, C., *Principles and Practice of Biological Mass Spectrometry*. Wiley Interscience: New York, 2001.

19. Hipple, J. A.; Sommer, H.; Thomas, H. A., A Precise Method of Determining the Faraday by Magnetic Resonance. *Physical Review* **1949,** *76* (12), 1877-1878.

20. Comisaro.Mb; Marshall, A. G., Fourier-Transform Ion-Cyclotron Resonance Spectroscopy. *Chem Phys Lett* **1974,** *25* (2), 282-283.

21. Lane, C. S., Mass spectrometry-based proteomics in the life sciences. *Cellular and molecular life sciences : CMLS* **2005,** *62* (7-8), 848-69.

22. Russell, D. H.; Smith, D. H.; Warmack, R. J.; Bertram, L. K., The design and performance evaluation of a new high-performance mass-analyzed ion kinetic energy (MIKE) spectrometer. *International Journal of Mass Spectrometry and Ion Physics* **1980,** *35* (3–4), 381-391.

23. McLafferty, F. W.; Todd, P. J.; McGilvery, D. C.; Baldwin, M. A., High-Resolution Tandem Mass Spectrometer (MS/MS) of Increased Sensitivity and Mass Range. *Journal of the American Chemical Society* **1980,** *102* (10), 3360-3363.

24. (a) Harrison, A. G.; Mercer, R. S.; Reiner, E. J.; Young, A. B.; Boyd, R. K.; March, R. E.; Porter, C. J., A hybrid BEQQ mass spectrometer for studies in gaseous ion chemistry. *Int J Mass Spectrom* **1986,** *74* (1), 13-31; (b) Schoen, A. E.; Amy, J. W.; Ciupek, J. D.; Cooks, R. G.; Dobberstein, P.; Jung, G., A hybrid BEQQ mass spectrometer. *Int J Mass Spectrom* **1985,** *65* (1–2), 125-140.

25. Campbell, J. M. C., B. A.; Douglas, D. J. A., New Linear Ion Trap Time-of-Flight System with Tandem Mass Spectrometry Capabilities. *Rapid Commun. Mass Spectrom.* **1998,** *12*, 1463-1474.

26. Morris, H. R.; Paxton, T.; Dell, A.; Langhorne, J.; Berg, M.; Bordoli, R. S.; Hoyes, J.; Bateman, R. H., High Sensitivity Collisionally-activated Decomposition Tandem Mass Spectrometry on a Novel Quadrupole/Orthogonal-acceleration Time-of-flight Mass Spectrometer. *Rapid Communications in Mass Spectrometry* **1996,** *10* (8), 889-896.

27. Yost, R. A.; Enke, C. G., Selected ion fragmentation with a tandem quadrupole mass spectrometer. *Journal of the American Chemical Society* **1978,** *100* (7), 2274-2275.

28. Ladislas Wiza, J., Microchannel plate detectors. *Nuclear Instruments and Methods 162* (1–3), 587-601.

29. Wysocki, V. H.; Tsaprailis, G.; Smith, L. L.; Breci, L. A., Special feature: Commentary - Mobile and localized protons: a framework for understanding peptide dissociation. *Journal of Mass Spectrometry* **2000,** *35* (12), 1399-1406.

30. Dongre, A. R.; Jones, J. L.; Somogyi, A.; Wysocki, V. H., Influence of peptide composition, gas-phase basicity, and chemical modification on fragmentation efficiency: Evidence for the mobile proton model. *Journal of the American Chemical Society* **1996,** *118* (35), 8365-8374.

31. Rodriquez, C. F.; Cunje, A.; Shoeib, T.; Chu, I. K.; Hopkinson, A. C.; Siu, K. W. M., Proton migration and tautomerism in protonated triglycine. *Journal of the American Chemical Society* **2001,** *123* (13), 3006-3012.

32. Paizs, B.; Suhai, S., Fragmentation pathways of protonated peptides. *Mass Spectrometry Reviews* **2005,** *24* (4), 508-548.

33. (a) Biemann, K., Contributions of Mass-Spectrometry to Peptide and Protein-Structure. *Biomed Environ Mass* **1988,** *16* (1-12), 99-111; (b) Roepstorff, P.; Fohlman, J., Proposal for a Common Nomenclature for Sequence Ions in Mass-Spectra of Peptides. *Biomed Mass Spectrom* **1984,** *11* (11), 601-601.

34. (a) Cooper, H. J.; Hakansson, K.; Marshall, A. G., The role of electron capture dissociation in biomolecular analysis. *Mass Spectrom Rev.* **2005,** *24* (2), 201-22; (b) Zubarev, R. A. K., N. L.; McLafferty, F. W, Electron Capture Dissociation of Multiply Charged Protein Cations. A Nonergodic Process. *J. Am. Chem. Soc.* **1998,** *120*, 3265-3266.

35. (a) Paizs, B.; Lendvay, G.; Vékey, K.; Suhai, S., Formation of b2+ ions from protonated peptides: an ab initio study. *Rapid Communications in Mass Spectrometry* **1999,** *13* (6), 525-533; (b) Polce, M. J.; Ren, D.; Wesdemiotis, C., Dissociation of the peptide bond in protonated peptides. *Journal of Mass Spectrometry* **2000,** *35* (12), 1391-1398; (c) Yalcin, T.; Csizmadia, I. G.; Peterson, M. R.; Harrison, A. G., The structure and fragmentation of B-n (n>=3) ions in peptide spectra. *Journal of the American Society for Mass Spectrometry* **1996,** *7* (3), 233-242; (d) Yalcin, T.; Khouw, C.; Csizmadia, I. G.; Peterson, M. R.; Harrison, A. G., Why are B ions stable species in peptide spectra? *Journal of the American Society for Mass Spectrometry* **1995,** *6* (12), 1165-1174.

36. Cordero, M. M.; Houser, J. J.; Wesdemiotis, C., The Neutral Products Formed during Backbone Fragmentations of Protonated Peptides in Tandem Mass-Spectrometry. *Anal Chem* **1993,** *65* (11), 1594-1601.

37. Bleiholder, C.; Osburn, S.; Williams, T. D.; Suhai, S. n.; Van Stipdonk, M.; Harrison, A. G.; Paizs, B. l., Sequence-Scrambling Fragmentation Pathways of Protonated Peptides. *Journal of the American Chemical Society* **2008,** *130* (52), 17774-17789.

38. Tang, X. J.; Boyd, R. K., An Investigation of Fragmentation Mechanisms of Doubly Protonated Tryptic Peptides. *Rapid Communications in Mass Spectrometry* **1992,** *6* (11), 651-657.

39. Yague, J.; Paradela, A.; Ramos, M.; Ogueta, S.; Marina, A.; Barahona, F.; de Castro, J. A. L.; Vazquez, J., Peptide rearrangement during quadrupole ion trap fragmentation: Added complexity to MS/MS spectra. *Anal Chem* **2003,** *75* (6), 1524-1535.

40. Tabb, D. L. S., L. L.; Breci, L. A.; Wysocki, V. H.; Lin, D.; Yates, J. R., Statistical Characterization of Ion Trap Tandem Mass Spectra from Doubly Charged Tryptic Peptides. *Anal. Chem.* **2003,** *75* (5), 1155-1163.

41. Savitski, M.; Fälth, M.; Eva Fung, Y. M.; Adams, C.; Zubarev, R., Bifurcating fragmentation behavior of gas-phase tryptic peptide dications in collisional activation. *Journal of the American Society for Mass Spectrometry* **2008,** *19* (12), 1755-1763.

42. Bythell, B. J.; Somogyi, Á.; Paizs, B., What is the Structure of b2 Ions Generated from Doubly Protonated Tryptic Peptides? *Journal of the American Society for Mass Spectrometry* **2009,** *20* (4), 618-624.

43. Harrison, A. G., Charge-separation reactions of doubly-protonated peptides: effect of peptide chain length. *Journal of the American Society for Mass Spectrometry* **2009,** *20* (10), 1890-5.

44. Knapp-Mohammady, M.; Young, A. B.; Paizs, B.; Harrison, A. G., Fragmentation of Doubly-Protonated Pro-His-Xaa Tripeptides: Formation of b_2^{2+} Ions. *Journal of the American Society for Mass Spectrometry* **2009,** *20* (11), 2135-2143.

45. Harrison, A. G., Effect of proline position on symmetric versus asymmetric fragmentation of doubly-protonated tryptic-type peptides. *International Journal of Mass Spectrometry* **2011,** *306* (2-3), 182-186.

46. Harrison, A. G., Effect of the Identity of Xaa on the Fragmentation Modes of Doubly-Protonated Ala-Ala-Xaa-Ala-Ala-Ala-Arg. *Journal of the American Society for Mass Spectrometry* **2011,** *22* (5), 906-911.

47. Li, X.; Huang, Y.; O'Connor, P.; Lin, C., Structural Heterogeneity of Doubly-Charged Peptide b-Ions. *Journal of the American Society for Mass Spectrometry* **2011,** *22* (2), 245-254.

48. Kilpatrick, L.; Neta, P.; Yang, X.; Simón-Manso, Y.; Liang, Y.; Stein, S., Formation of y + 10 and y + 11 Ions in the Collision-Induced Dissociation of Peptide Ions. *Journal of the American Society for Mass Spectrometry* **2012,** *23* (4), 655-663.

49. Huang, Y. Y.; Wysocki, V. H.; Tabb, D. L.; Yates, J. R., The influence of histidine on cleavage C-terminal to acidic residues in doubly protonated tryptic peptides. *International Journal of Mass Spectrometry* **2002,** *219* (1), 233-244.

50. Tsaprailis, G.; Nair, H.; Zhong, W.; Kuppannan, K.; Futrell, J. H.; Wysocki, V. H., A mechanistic investigation of the enhanced cleavage at histidine in the gas-phase dissociation of protonated peptides. *Anal Chem* **2004,** *76* (7), 2083-2094.

51. Paradela, A. G.-P., M.; Vazquez, J.; Rognan, D.; Lopez de Castro, J. A., The Same Nautral Ligand is Involved in Allorecognition of Multiple HLA-B27 Subtypes by a Single T Cell Clone: Role of Peptide and the MHC Molecule in Allreactivity *J Immunol* **1998,** *161,* 5481-5490.